

UNCLASSIFIED

AD NUMBER
AD885919
NEW LIMITATION CHANGE
TO Approved for public release, distribution unlimited
FROM Distribution authorized to U.S. Gov't. agencies and their contractors; Critical Technology; MAY 1972. Other requests shall be referred to Air Force Avionics Lab., Wright-Patterson AFB, OH 45433.
AUTHORITY
AFAL ltr, 4 Oct 1973

THIS PAGE IS UNCLASSIFIED

2

NEODYMIUM APOPTIC LIQUID LASER

J. D. Foster

R. F. Kirk

GTE Sylvania
ELECTRO-OPTICS ORGANIZATION
Mountain View, California

TECHNICAL REPORT AFAL-TR-71-122

May 1971

This document is subject to special export controls and each transmittal to foreign governments or foreign nationals may be made only with prior approval of Air Force Avionics Laboratory. /TEL

W-P- AFB, Ohio #5433

AD885919

AD No. FILE COPY



DDC
RECORDED
JUL 29 1971
REGULATED
C

Air Force Avionics Laboratory
Air Force Systems Command
Wright-Patterson Air Force Base, Ohio

73

UNCLASSIFIED

Security Classification

DOCUMENT CONTROL DATA - R&D		
<i>(Security classification of title, body of abstract and indexing annotation must be entered when the overall report is classified)</i>		
1. ORIGINATING ACTIVITY (Corporate author) GTE Sylvania, Inc., Electro-Optics Organization Electronic Systems Division, P.O. Box 188 Mountain View, California 94040		2a. REPORT SECURITY CLASSIFICATION UNCLASSIFIED
		2b. GROUP
3. REPORT TITLE NEODYMIUM APROTIC LIQUID LASER		
4. DESCRIPTIVE NOTES (Type of report and inclusive dates) FINAL TECHNICAL REPORT 16 February 1970 through 16 March 1971		
5. AUTHOR(S) (Last name, first name, initial) FOSTER, Jack D. and KIRK, Russell F.		
6. REPORT DATE May 1971	7a. TOTAL NO. OF PAGES	7b. NO. OF REFS
8a. CONTRACT OR GRANT NO. F33615-70-C-1415	8a. ORIGINATOR'S REPORT NUMBER(S)	
b. PROJECT NO. 5237		
c.	8b. OTHER REPORT NO(S) (Any other numbers that may be assigned this report)	
d.	AFAL-TR-71-122	
10. AVAILABILITY/LIMITATION NOTICES ●		
11. SUPPLEMENTARY NOTES	12. SPONSORING MILITARY ACTIVITY AF Avionics Laboratory (AFAL/TEL) Wright-Patterson AFB, Ohio 45433	
13. ABSTRACT This report describes the results of a research and development program directed at achieving high average power operation from a transverse flow Nd:POCl ₃ ;ZrCl ₄ liquid laser. Theoretical calculation of expected performance predicted over 50 joules long pulse output at greater than 3 percent efficiency. Transverse flow was expected to allow operation at 10 Hz and higher. A flowing system was designed using materials compatible with the corrosive liquid. Many problems were encountered in getting a leak-free assembly with these limited materials. The flowing system was filled, outgassed and operated. Problems of scattering in the liquid, corrosion of critical laser components by the corrosive POCl ₃ vapor and breakage severely limited the results obtained. Q-switched operation at 4 to 8 MW peak power and 45 nsec pulse width was obtained. Single shot, 300 μsec width pulsed output energies of 12 joules were obtained at around 0.37 percent efficiency. Threshold was just obtained at 10 Hz. The conclusion is reached that materials problems with transverse flow are so great that simpler longitudinal flow systems should be developed before further development of transverse flow.		

DD FORM 1473
1 JAN 64

67.

UNCLASSIFIED

Security Classification

NOTICE

When Government drawings, specifications, or other data are used for any purpose other than in connection with a definitely related Government procurement operation, the United States Government thereby incurs no responsibility nor any obligation whatsoever; and the fact that the government may have formulated, furnished, or in any way supplied the said drawings, specifications, or other data, is not to be regarded by implication or otherwise as in any manner licensing the holder or any other person or corporation, or conveying any rights or permission to manufacture, use, or sell any patented invention that may in any way be related thereto.

ACCESSION NO.		
WPBT	WHITE SECTION <input type="checkbox"/>	
ACC	BWF SECTION <input checked="" type="checkbox"/>	
UNANNOUNCED	<input type="checkbox"/>	
JUSTIFICATION		
BY		
DISTRIBUTION/AVAILABILITY CODE		
GEN.	AVAIL. 301/12	SPECIAL
2		

Copies of this report should not be returned unless return is required by security considerations, contractual obligations, or notice on a specific document.

14 KEY WORDS	LINK A		LINK B		LINK C	
	ROLE	WT	ROLE	WT	ROLE	WT
Laser						
Neodymium Laser						
Liquid Laser						

INSTRUCTIONS

1. **ORIGINATING ACTIVITY:** Enter the name and address of the contractor, subcontractor, grantee, Department of Defense activity or other organization (*corporate author*) issuing the report.

2a. **REPORT SECURITY CLASSIFICATION:** Enter the overall security classification of the report. Indicate whether "Restricted Data" is included. Marking is to be in accordance with appropriate security regulations.

2b. **GROUP:** Automatic downgrading is specified in DoD Directive 5200.10 and Armed Forces Industrial Manual. Enter the group number. Also, when applicable, show that optional markings have been used for Group 3 and Group 4 as authorized.

3. **REPORT TITLE:** Enter the complete report title in all capital letters. Titles in all cases should be unclassified. If a meaningful title cannot be selected without classification, show title classification in all capitals in parenthesis immediately following the title.

4. **DESCRIPTIVE NOTES:** If appropriate, enter the type of report, e.g., interim, progress, summary, annual, or final. Give the inclusive dates when a specific reporting period is covered.

5. **AUTHOR(S):** Enter the name(s) of author(s) as shown on or in the report. Enter last name, first name, middle initial. If military, show rank and branch of service. The name of the principal author is an absolute minimum requirement.

6. **REPORT DATE:** Enter the date of the report as day, month, year, or month, year. If more than one date appears on the report, use date of publication.

7a. **TOTAL NUMBER OF PAGES:** The total page count should follow normal pagination procedures, i.e., enter the number of pages containing information.

7b. **NUMBER OF REFERENCES:** Enter the total number of references cited in the report.

8a. **CONTRACT OR GRANT NUMBER:** If appropriate, enter the applicable number of the contract or grant under which the report was written.

8b, 8c, & 8d. **PROJECT NUMBER:** Enter the appropriate military department identification, such as project number, subproject number, system numbers, task number, etc.

9a. **ORIGINATOR'S REPORT NUMBER(S):** Enter the official report number by which the document will be identified and controlled by the originating activity. This number must be unique to this report.

9b. **OTHER REPORT NUMBER(S):** If the report has been assigned any other report numbers (either by the originator or by the sponsor), also enter this number(s).

10. **AVAILABILITY/LIMITATION NOTICES:** Enter any limitations on further dissemination of the report, other than those

imposed by security classification, using standard statements such as:

- (1) "Qualified requesters may obtain copies of this report from DDC."
- (2) "Foreign announcement and dissemination of this report by DDC is not authorized."
- (3) "U. S. Government agencies may obtain copies of this report directly from DDC. Other qualified DDC users shall request through _____."
- (4) "U. S. military agencies may obtain copies of this report directly from DDC. Other qualified users shall request through _____."
- (5) "All distribution of this report is controlled. Qualified DDC users shall request through _____."

If the report has been furnished to the Office of Technical Services, Department of Commerce, for sale to the public, indicate this fact and enter the price, if known.

11. **SUPPLEMENTARY NOTES:** Use for additional explanatory notes.

12. **SPONSORING MILITARY ACTIVITY:** Enter the name of the departmental project office or laboratory sponsoring (paying for) the research and development. Include address.

13. **ABSTRACT:** Enter an abstract giving a brief and factual summary of the document indicative of the report, even though it may also appear elsewhere in the body of the technical report. If additional space is required, a continuation sheet shall be attached.

It is highly desirable that the abstract of classified reports be unclassified. Each paragraph of the abstract shall end with an indication of the military security classification of the information in the paragraph, represented as (TS), (S), (C), or (U).

There is no limitation on the length of the abstract. However, the suggested length is from 150 to 225 words.

14. **KEY WORDS:** Key words are technically meaningful terms or short phrases that characterize a report and may be used as index entries for cataloging the report. Key words must be selected so that no security classification is required. Identifiers, such as equipment model designation, trade name, military project code name, geographic location, may be used as key words but will be followed by an indication of technical context. The assignment of links, rules, and weights is optional.

NEODYMIUM APROTIC LIQUID LASER

J. D. Foster

R. F. Kirk

GTE SYLVANIA, INCORPORATED

May 1971

FOREWORD

This is the final Technical Report on a research and development program conducted by the GTE Sylvania, Inc. Electro-Optics Organization, Mountain View, California, under U. S. Air Force Systems Command, Contract No. F33615-70-C-1415, Project 5237. This work is being administered by the Air Force Avionics Laboratory, Air Force Systems Command, Wright-Patterson Air Force Base, Ohio. The Air Force Program Monitor is David L. Flannery. Dr. J. D. Foster is the principal investigator for GTE Sylvania, Inc. This report was submitted by the authors on 1 April 1971.

This technical report has been reviewed and is approved for publication.

Amos H. Dicke
AMOS H. DICKE
Chief, Laser Technology Branch
Electronic Technology Division

ABSTRACT

This report describes the results of a research and development program directed at achieving high average power operation from a transverse flow Nd:POCl₃:ZrCl₄ liquid laser. Theoretical calculation of expected performance predicted over 50 joules long pulse output at greater than 3 percent efficiency. Transverse flow was expected to allow operation at 10 Hz and higher.

A flowing system was designed using materials compatible with the corrosive liquid. Many problems were encountered in getting a leak-free assembly with these limited materials.

The flowing system was filled, outgassed and operated. Problems of scattering in the liquid, corrosion of critical laser components by the corrosive POCl₃ vapor and breakage severely limited the results obtained.

Q-switched operation at 4 to 8 MW peak power and 45 nsec pulse width was obtained. Single shot, 300 μsec width pulsed output energies of 12 joules were obtained at around 0.37 percent efficiency. Threshold was just obtained at 10 Hz.

The conclusion is reached that materials problems with transverse flow are so great that simpler longitudinal flow systems should be developed before further development of transverse flow.

<u>SECTION</u>	<u>Title</u>	<u>Page</u>
1.	INTRODUCTION	1
2.	THEORETICAL MODEL	7
2.1	Continuous Operation of the Nd:POCl ₃ Laser	14
2.2	Long Pulse Operation of the Nd:POCl ₃ Laser	14
2.3	Q-Switched Operation of the Nd:POCl ₃ Laser	18
3.	FLOWING LIQUID LASER DESIGN	21
3.1	Laser Cell Design	21
3.2	Liquid Laser Circulation	23
3.2.1	Heat Exchanger	32
3.2.2	Pump	35
3.3	Power Supply	37
3.4	Q-Switching	41
4.	ASSEMBLY AND FILLING OF THE LIQUID LASER	47
4.1	Assembly Procedure	47
4.2	Filling Procedure	49
5.	EXPERIMENTAL RESULTS	51
5.1	First Series of Experiments	51
5.2	Second Series of Experiments	53
6.	CONCLUSIONS AND RECOMMENDATIONS	61
7.	REFERENCES	65

LIST OF ILLUSTRATIONS

<u>Figure</u>	<u>Title</u>	<u>Page</u>
2-1	Estimated CW Performance of the Nd:POCl ₃ Liquid Laser	15
2-2	Pulsed Laser Input/Output Data for Nd:YAG and Nd:Glass at 2 pps	16
2-3	Estimated Long Pulse Performance of the Nd:POCl ₃ :ZrCl ₄ Liquid Laser	19
3-1	Cross Section of Liquid Laser Cell	22
3-2	Hydrodynamic Model of the Transverse Flow Liquid Laser Cell	24
3-3	Twyman/Green Interferometer for Measuring Optical Distortion in the Laser Liquid Cell.	25
3-4	Liquid Pumping Arrangement	26
3-5	Twyman/Green Interferometer Fringes Through Model Liquid Laser with Flowing Water - Ethylene Glycol Mixture Matching Reynolds Number of POCl ₃	27
3-6	Flow Diagram for the Liquid Laser	28
3-7	Liquid Laser Circulation System	30
3-8	Liquid Laser System	31
3-9	Liquid Laser Heat Exchanger Core and Pressure Compensation Piston	36
3-10	Face Seal Schematic for Liquid Laser Pump	38
3-11	Pump Characteristics and System Load Line for Liquid Laser System	39
3-12	Liquid Laser Power Supply	40
3-13	Liquid Laser Lamp Firing Circuit	42
3-14	Mechanical Q-Switching Arrangements for the Liquid Laser	43
3-15	Rotating Porro Prism Mechanical Q-Switch	44
3-16	Rotating Brewster's Angle Total Internal Reflecting Prism Mechanical Q-Switch	45
4-1	Assembly of the Transverse Flow Liquid Laser Cell	48
5-1	Long Pulse (300 μsec) Static Liquid Laser Results	52
5-2	Liquid Laser System in Second Series of Experiments	55

LIST OF ILLUSTRATIONS (CONTINUED)

<u>Figure</u>	<u>Title</u>	<u>Page</u>
5-3	Rotating Roof Prism Q-Switch Results for Nd:POCl ₃ Liquid Laser. Scale is 4 MW/cm Vertical and 2 μsec/cm Horizontal. Increasing Time for Left to Right.	56
5-4	Rotating Roof Prism Q-switch Results for Nd:POCl ₃ Liquid Laser. Scale is 2 MW/cm Vertical and 1 μsec/cm Horizontal. Increasing Time from Left to Right.	56
5-5	Long Pulse Results for Nd:POCl ₃ Liquid Laser. Scale in Relative Units Vertical and 50 ³ μsec/cm Horizontal. Time Increases from Left to Right.	57
5-6	Corroded Pump Cavity Reflectors Due to POCl ₃ Vapor Leakage in Liquid Leak Free System	59
6-1	Pump Characteristics and System Load Line for Longitudinal Flow and Transverse Flow Systems	62

LIST OF TABLES

<u>Table No.</u>	<u>Title</u>	<u>Page</u>
2-1	Laser Parameters for Nd:YAG, Nd:ED-2 Glass and Nd:POCl ₃ :ZrCl ₄	13
2-2	Peak Power Densities for Damage of Various Materials and for Onset of Significant Nonlinear Effects in POCl ₃ Cell 30 cm Long	20

1. INTRODUCTION

The laser has important military applications in illumination, target designation, ranging, and tracking. Many of these applications require high energy pulses of short time duration and high repetition rate.

The most successful laser sources for these applications have used the infrared Nd^{+3} emission at 1.06 microns. Three types of host materials, crystalline, glass, and liquid have been successfully employed. Each of these has special characteristics.

Crystalline hosts such as yttrium - aluminum-garnet (YAG) and yttrium orthoaluminate (YAlO_3) are capable of only low pulse energies because of their limited energy storage capacity. Crystalline laser rods are limited to small sizes by crystal growth limitations. Thermal distortions limit the mode purity of the laser output and thermal stress limits the average power output. The high thermal conductivity of crystalline materials does allow high repetition rate operation at moderate pulse energies and fairly high average powers.

Glass hosts are capable of high pulse energies because of their large energy storage capability. They have the thermal distortion and stress of all solid lasers. Low thermal conductivity seriously limits the mode purity and average power capabilities. Techniques to improve heat dissipation by segmenting the glass rods are under development. Glass lasers can produce high pulse energies at low and possibly moderately high repetition rates and average powers.

Liquid hosts for Nd offer a way to achieve pulse energies intermediate between those of crystalline and glass lasers at high average powers. The essentially unlimited size possible with liquid host materials offers the capability for continued improvement in output power and energy as successful liquid laser techniques are developed.

Lasers based upon the liquid phase of matter have lagged somewhat behind solid and gas lasers in their rate of development. The reason for this

has been primarily the detrimental effect of the hydrogen on fluorescent lifetimes in liquids. Solutions to this problem have followed two paths. First, fluorescent compounds were developed that shield the fluorescence site from the solvent; examples are chelate lasers and dye lasers. The second path has been to use inorganic non-hydrogen-containing ("aprotic," without protons) liquids for the solvent.

Heller,¹ at GTE Laboratories, discovered the requirement for aprotic liquids. Shortly after this, Lempicki and Heller² built the first inorganic liquid laser. This laser utilized SeOCl_2 made into a Lewis acid with SnCl_4 as a solvent for Nd^{3+} . The GTE Laboratories group has built a number of very interesting lasers based upon SeOCl_2 , but this material has never been widely used because it is very toxic and very corrosive.

A number of nontoxic aprotic compounds were investigated by GTE Laboratories; however, difficulty was experienced in dissolving Nd into the solutions. On a trip to Russia in 1967, Lempicki found that POCl_3 was being used in large quantities as a liquid laser medium for neodymium. In recent publications,^{3,4} the Russian investigators describe some of their laser results. The only hint they give on liquid preparation is the statement:

"We discovered and investigated the condensation and polycondensation reactions of rare-earth compounds with phosphorous oxychloride in the presence of multivalent metal halides. Solutions of rare-earth ions with good physicochemical and luminescent properties are obtained as a result of the reactions."

Following this trip, GTE Laboratories was able to dissolve Nd in $\text{POCl}_3:\text{SnCl}_4$ by adding water and then distilling the water off. The resultant laser liquid was never really stable but had good short term laser properties.

Schimitschek at the Naval Electronics Laboratory Center, San Diego, California, investigated chemical reactions of neodymium compounds with various Lewis acids of POCl_3 . At first,⁵ he used $\text{Nd}(\text{ClO}_4)_3$ but found the solutions

not to be stable. He then found⁶ that $\text{Nd}(\text{CF}_3\text{COO})_3$, when reacted with the Lewis acid of POCl_3 formed with ZrCl_4 , put the Nd in solution, with the evolution of CF_3COCl gas. The solution thus formed was found to be very stable, and to be somewhat less corrosive than SeOCl_2 . It has become the primary liquid laser solution in this country. The similarity of Schimitschek's reaction and the Russian's discussion of their reaction should be noted.

The Russians quote^{3,4} some performance data on their liquid laser. They have achieved outputs of 350 joules and efficiencies up to 1 percent. They have found the laser liquid to be stable, with thousands of flashes at energies exceeding 10 J/cm^3 absorption into the pump bands producing no noticeable deterioration of the liquid. In Reference 3, they show a photograph of the 350J liquid laser. It has 6 pump lamps in a cylindrical pump cavity and provisions for flowing the liquid are visible.

At GTE Labs, a maximum pulsed output of 44 joules⁷ has been obtained at 2.7 percent overall efficiency from a $\text{Nd}:\text{POCl}_3:\text{SnCl}_4$ liquid cell of 74 cm^3 (1.95 cm Dia x 25 cm). This represents an output of 0.6 joules/cm^3 or a much lower output energy per unit volume and higher efficiency than the Russians.

GTE Labs has expended a considerable amount of effort on flowing liquid laser systems.^{8,9,10} They have achieved¹⁰ 60 watts average output power at 5 pps repetition rate.

The development of a nontoxic liquid laser material, coupled with the knowledge of liquid laser materials and techniques that have been developed, provides a basis from which to build high power liquid lasers. Most of the work prior to 1969 has been of a scientific nature. It was recognized in 1969 that the technology for building an engineering prototype high-energy liquid laser was at hand. In August 1969, GTE Sylvania's Electro-Optics Organization started a GTE Corporation sponsored 6-month engineering effort to build such a laser. The project was a cooperative effort with GTE Laboratories and was funded through them. Sylvania EOO engineers were instructed in all aspects of liquid laser technology by GTE Laboratories. Sylvania engineers then proceeded to design an engineering prototype liquid laser. This design was based upon the solid state

laser¹¹ and gas transport laser¹² expertise at Sylvania, as well as the liquid technology. The resulting design was reviewed with GTE Labs and then constructed. Assembly and testing of the prototype laser was accomplished on Air Force Contract F33615-70-C-1415. This is the final report for this contract.

The objectives of this program were to design, construct, test, and analyze the performance of a high-average-power liquid laser in three modes of operation. In the long-pulse mode, the objective was 50 joules per pulse at 10 pps. In a Q-switched mode, 2.5 joules at 10 pps was desired. The emphasis of the program was to attain maximum energy in a Q-switched pulse. Finally, CW operation at the 500 watt output level was to be attempted. The circulation system was to be closed and circulation accomplished with a mechanical pump. The liquid was to consist of phosphorous oxychloride with appropriate agents for introducing Nd^{+3} ions into solution.

The following tasks were to be accomplished:

a. Circulatory System

Design a circulatory system consisting of a laser head, mechanical pump, and a heat exchanger using materials that are resistant to the corrosive properties of POCl_3 . The nature of the liquid flow, i.e., transverse or axial, laminar or turbulent, will be conducive to optimum optical quality. It is desirable to be able to measure the rate of flow and qualitatively describe the velocity profile in the laser cell.

b. Optical Pump Cavity

An optical pump cavity will be designed which allows adequate provision for laser liquid circulation and lamp cooling, and also gives good optical coupling.

c. Q-Switching

Electro-optic and mechanical Q-switch devices will be used with the 10 pps, high-average-power laser with the objective of 2.5 joules per pulse or higher. Parameters which are of most interest are energy, beam divergence, and efficiency. The emphasis of the program is to be on optimizing the Q-switching performance of the laser.

2. THEORETICAL MODEL

It is necessary to outline the theoretical model of Nd lasers in order to clearly predict the performance of Nd:Liquid lasers. For a homogeneously broadened medium the single pass gain experienced by photons traversing the optically pumped laser medium is given by¹³

$$g = g_0 \left(\frac{1}{1 + \beta P_{\text{cir}}} \right) \quad (2-1)$$

where

g = the saturated single pass gain

g_0 = the unsaturated single pass gain

β = a saturation parameter

P_{cir} = the optical power traversing the laser medium (one direction).

Let us restrict our discussion to the CW laser case for a while and generalize the results to the pulsed case later.

If measurements are made of g_0 for a given pump lamp and pump cavity we find that phenomenologically

$$g_0 = K(P - P_0) \quad (2-2)$$

to very good approximation where

K = constant

P = input power to pump lamp

P_0 = intercept of linearized lamp output versus input data
(physically the heat loss of the lamp).

In a laser oscillator with single pass dissipative loss, α_0 , and transmission loss, T , only through one laser mirror, the single pass loss

for the laser, α , is

$$\alpha = \alpha_0 + \frac{T}{2} \quad (2-3)$$

The output power P_{out} is

$$P_{out} = T P_{cir} \quad (2-4)$$

Substituting Equation (2-2) into (2-1), setting gain equal to loss for the laser oscillation condition by setting Equation (2-1) equal to Equation (2-3), and substituting into Equation (2-4), we obtain

$$P_{out} = \frac{T}{\beta} \left[\frac{K(P - P_0)}{\alpha} - 1 \right]$$

$$P_{out} = \frac{TK}{\beta\alpha} \left[P - \left(P_0 + \frac{\alpha}{K} \right) \right] \quad (2-5)$$

Laser performance is usually shown on a power output versus power input plot with two parameters, the threshold P_{th} and the slope efficiency η_d

From Equation (2-5) we see that expressions for P_{th} and η_d are

$$P_{th} = P_0 + \frac{\alpha}{K}$$

$$\eta_d = \frac{TK}{\beta\alpha} \quad (2-6)$$

If we start with a set of four level rate equations⁽²⁷⁾ and make a number of simplifying assumptions appropriate for neodymium, we can arrive at the following set of coupled rate equations

$$\frac{dN}{dt} = WN_1 \eta - 2c\sigma\tau N - \frac{2N}{\tau_{tot}}$$

$$\frac{dJ}{dt} = c\sigma\tau N + \frac{nN}{p\tau_i} - \frac{J}{\tau_c} \quad (2-7)$$

where

- N = the number of inverted ions per unit volume in the laser material
- ζ = the number of photons per unit volume stored in the laser resonator
- WN_1 = the pumping rate into the laser pump bands per unit volume
- N_1 = the number of laser ions per unit volume in the ground state
- η = the average quantum efficiency of the pump bands
- c = velocity of light
- σ = cross section for stimulated emission in the laser material
- τ_{tot} = the total lifetime of the upper laser level for spontaneous emission
- τ_l = the spontaneous lifetime of the upper laser level only for the laser transition
- $\tau_c = \frac{L}{ca}$, the lifetime of a photon in the laser resonator cavity
- n = the number of oscillating laser modes
- p = the number of modes in the laser resonant cavity that can couple to the fluorescent line
- L = laser resonator length
- α = the single pass loss in the laser resonant cavity.

Solving these coupled rate equations for the steady state case, $dN/dt = d\zeta/dt = 0$, we find

$$P_{\text{out}} = \frac{T}{\frac{2\sigma\tau_{\text{tot}}}{Ah\nu}} \left[\frac{WN_1\eta\sigma\tau_{\text{tot}}L}{2\alpha} - 1 \right] \quad (2-8)$$

where

T = the transmission of the laser mirrors

A = the cross sectional area of the laser material.

We must have a model for the pumping rate WN_1 . Let us assume that pump band radiation is emitted proportional to $P - P_0$ where P is the input power to the pump lamp and P_0 is the heat loss.

Assume that we have an efficient pump cavity that directs all the light from the pump lamp to the laser material. The intensity of light at the surface of the cylindrical laser material will then be

$$I = \frac{K}{Ld} (P - P_0) \quad (2-9)$$

where

d = the laser rod diameter

K = a constant of proportionality which reflects efficiency of the pump lamp and pump cavity for providing radiation in the pump bands.

Let us now assume that the laser material is on the average optically thin so that we may take I as the pump radiation intensity throughout the laser material. The pumping rate per unit volume is then:

$$WN_1 = \sigma_p I N_1 = \frac{2k N_1}{Ld} (P - P_0) \quad (2-10)$$

where

σ_p = the average cross section for pumping

$$k = \frac{\sigma_p K}{2}$$

Substituting Equation (2-10) into Equation (2-8)

$$P_{\text{out}} = \frac{T}{\frac{2\sigma\tau_{\text{tot}}}{Ah\nu}} \left[\frac{\frac{kN_1 \eta (P-P_0) \sigma\tau_{\text{tot}}}{d}}{\alpha} - 1 \right] \quad (2-11)$$

Comparing Equation (2-11) with Equation (2-5) we see that we have developed scaling laws for the constants in Equation (2-5) in terms of the laser material properties

$$\beta = \frac{2\sigma\tau}{h\nu A}$$

$$K = \frac{k \eta \sigma \tau_{\text{tot}} N_1}{d} \quad (2-12)$$

• •

Substituting into Equation (2-6)

$$\begin{aligned} P_{\text{th}} &= P_0 + \frac{\alpha d}{k \eta \sigma \tau_{\text{tot}} N_1} \\ \eta_d &= \frac{T k \eta N_1 h\nu A}{2d\alpha} \end{aligned} \quad (2-13)$$

Equations (2-13) express the threshold and slope efficiency for continuous lasers. We can use these equations to predict continuous performance of the liquid laser based upon results with the Nd:YAG laser.

Time dependent analysis of pulsed lasers is very difficult and depends upon the time history of the pump pulse. A good approximation can be made by assuming steady state (or average) conditions during the pulse width. Most pulsed laser data is presented in output pulse energy versus input energy form. We convert our equations to pulse energies by multiplying the steady state power by the pulse width.

For pulsed lasers, Equation (2-5) becomes

$$E_{\text{out}} = \frac{TK}{\beta\alpha} \left[E - \left(E_0 + \frac{\alpha}{t_p K} \right) \right] \quad (2-14)$$

where

E_{out} = laser output pulse

E = laser input pulse energy

t_p = pulse width

$E_0 = P_0 t_p$ ($E_0 = 0.1\text{J}$ and may be neglected in most pulsed laser calculations)

Equations (2-6) become

$$E_{\text{th}} = E_0 + \frac{\alpha}{t_p K} \quad (2-15)$$

$$\eta_d = \frac{TK}{\beta\alpha}$$

Equations (2-13) become

$$\boxed{\begin{aligned} E_{\text{th}} &= E_0 + \frac{\alpha d}{k\eta\sigma_{\text{tot}} N_1 t_p} \\ \eta_d &= \frac{Tk\eta N_1 h\nu d}{2d\alpha} \end{aligned}} \quad (2-16)$$

It should be noted in Equations (2-13) and (2-16) that the threshold depends inversely upon the product of the upper state total lifetime and the cross section for stimulated emission $\tau_{\text{tot}}\sigma$ but the slope efficiency does not. The threshold depends inversely upon the pumping efficiency k , the quantum efficiency η , and the ion doping density N_1 . The slope efficiency varies directly with these factors. The threshold depends directly and the slope efficiency inversely upon the laser material diameter d .

These equations agree with what one would estimate from intuition. The variation with d is probably the most questionable because of effects of nonuniform absorption of pump radiation and multiple passes in the pump cavity. We have found the d variation to be approximately correct for scaling CW Nd:YAG rods of 0.15 inch and 0.25 inch diameter.

The pulsed laser equations are much more questionable than the CW because of the steady state assumption in the derivation.

In Table 2-1 we have collected estimated values for the various parameters for Nd:YAG, Nd:ED-2 Glass, and Nd:POCl₃:ZrCl₄.

Table 2-1. Laser Parameters for Nd:YAG, Nd:ED-2 Glass and Nd:POCl₃:ZrCl₄

MATERIAL	N_1 ions/cm ³	σ cm ²	τ Microsec	η	REFERENCE
Nd:YAG	1.4×10^{20}	5.7×10^{-19}	240	1.0	14, 15
Nd:ED-2 Glass	2.7×10^{20}	3×10^{-20}	300	0.5	14, 16
Nd:POCl ₃ :ZrCl ₄	1.8×10^{20}	6×10^{-20}	330	0.5	17

2.1 Continuous Operation of the Nd:POCl₃ Laser

Let us first consider CW operation of the Nd:POCl₃ liquid laser. The equations (2-13) are probably quite accurate for this case. The increase in the dissipative loss, α_0 , due to flow is difficult to forecast. We will lump this loss in with the scattering and absorption loss and will consider α_0 as a variable. From experimental measurements of Kr arc pumped Nd:YAG laser performance, Equations (2-13) and the laser parameters, we can estimate the CW performance of Nd:POCl₃ liquid lasers. We will assume a 3/4-inch diameter, 12-inch long Nd:POCl₃ laser cell pumped with a Kr arc with a rated power of 30 kW (these conform to our liquid laser design). The pump absorption bands of Nd:POCl₃ are more like those of Nd:Glass than those of Nd:YAG. We will assume $k_{\text{POCl}_3} / k_{\text{YAG}} = 1.6$ based upon pulsed experimental comparison of Nd:YAG and Nd:Glass.

The resulting prediction of laser output power as a function of dissipative loss in the laser liquid is shown in Figure 2-1. The strong dependence upon the loss should be noted. Present estimates of the loss in Nd:POCl₃:ZrCl₄ by GTE Labs is 0.16 percent per cm. If this is true, a continuous output of 900 W is predicted. There is, therefore, hope of very high power operation depending very much upon the scattering and absorption loss in the flowing laser liquid.

2.2 Long Pulse Operation of the Nd:POCl₃ Laser

Our basis for predicting the long pulse performance of the Nd:YAG is less accurate than was the CW due to the steady state assumption in deriving Equations (2-16). We do, however, have more experimental results on which to make predictions.

Let us consider a long pulse comparison of Nd:YAG with Nd:ED-2S Glass to check Equations (2-16). The experimental results are shown in Figure 2-2. Considering the threshold first and assuming $\alpha_{\text{Glass}} = \alpha_{\text{YAG}}$,

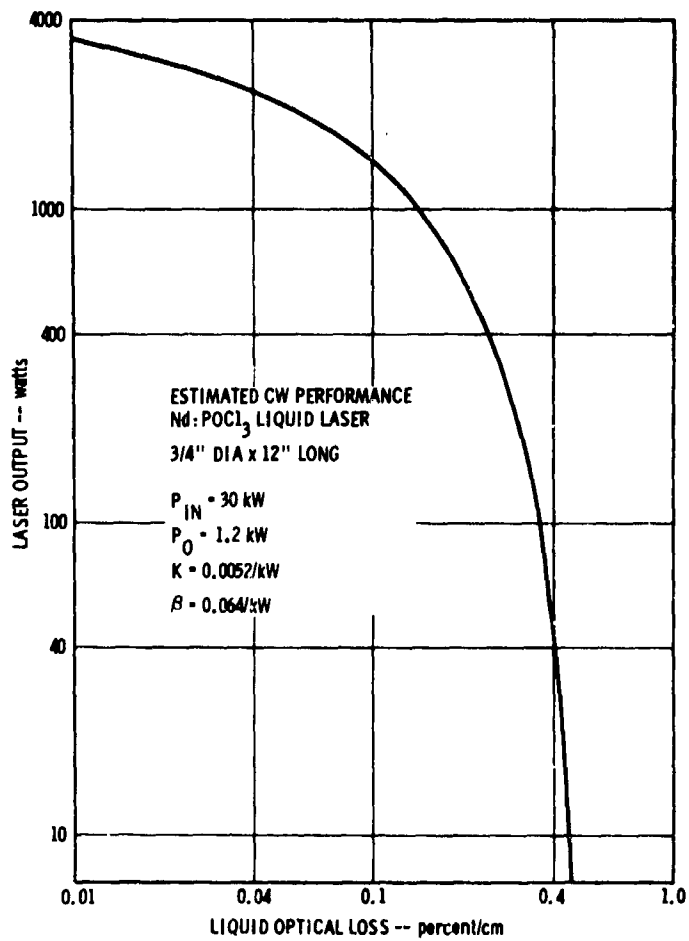


Figure 2-1. Estimated CW Performance of the Nd:POCl₃ Liquid Laser With Optimum Output Coupling

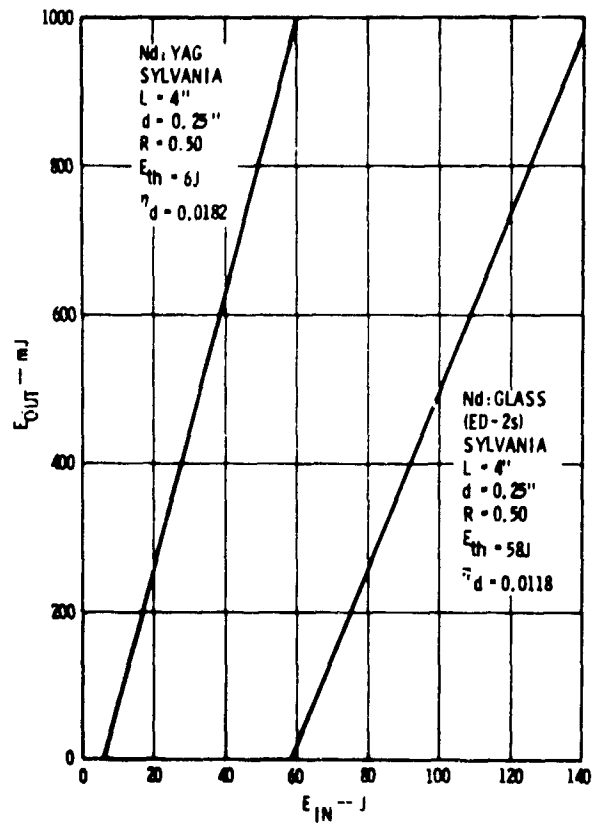


Figure 2-2. Pulsed Laser Input/Output Data for Nd:YAG and Nd:Glass at 2 pps

Equations (2-16) gives

$$\frac{E_{th \text{ Glass}}}{E_{th \text{ YAG}}} = \frac{k_{\text{YAG}}}{k_{\text{Glass}}} \frac{(\eta N_1 \sigma \tau_{tot})_{\text{YAG}}}{(\eta N_1 \sigma \tau_{tot})_{\text{Glass}}} = 15.5 \frac{k_{\text{YAG}}}{k_{\text{Glass}}}$$

The measured ratio of thresholds is 9.57. The value of $k_{\text{Glass}}/k_{\text{YAG}} = 1.6$ for the theory and experiment to agree. This seems like a reasonable ratio for the k's since the pump bands of the glass are wider than YAG. We conclude that the theory is accurate for the threshold prediction.

Considering the slope efficiency, Equations (2-16) predict

$$\frac{\eta_d \text{ Glass}}{\eta_d \text{ YAG}} = \frac{k_{\text{Glass}}}{k_{\text{YAG}}} \frac{(\eta N_1)_{\text{Glass}}}{(\eta N_1)_{\text{YAG}}} = 1.54$$

The experimentally measured value for the slope efficiency ratio was 0.65. We have a significant difference between theory and experiment. An estimated reason for this is that α is power dependent due to the greater thermal effects in Glass.

Let us now consider the predictions from Equations (2-16) for a 3/4-inch diameter by 12-inch Nd:POCl₃ liquid laser. Assume $k_{\text{POCl}_3}/k_{\text{YAG}} = 1.6$, $\alpha_{\text{POCl}_3} = 0.16$, $\alpha_{\text{YAG}} = 0.01$, and $T_{\text{POCl}_3} = 0.7$; and base the prediction on the 1/4-inch diameter Nd:YAG results shown in Figure 2-2. Then using equations (2-16) we have

$$E_{th}^{\text{POCl}_3} = \left(\frac{\alpha_{\text{POCl}_3}}{\alpha_{\text{YAG}}} \right) \left(\frac{d_{\text{POCl}_3}}{d_{\text{YAG}}} \right) \left(\frac{k_{\text{YAG}}}{k_{\text{POCl}_3}} \right) \frac{(\eta N_1 \sigma \tau_{tot})_{\text{YAG}}}{(\eta N_1 \sigma \tau_{tot})_{\text{POCl}_3}} E_{th}^{\text{YAG}} = 238 \text{ joules}$$

Similarly using Equations (2-6) to predict the slope efficiency

$$\eta_{d, \text{POCl}_3} = \left(\frac{T_{\text{POCl}_3}}{T_{\text{YAG}}} \right) \left(\frac{k_{\text{POCl}_3}}{k_{\text{YAG}}} \right) \left(\frac{d_{\text{POCl}_3}}{d_{\text{YAG}}} \right) \left(\frac{\alpha_{\text{YAG}}}{\alpha_{\text{POCl}_3}} \right) \frac{(\eta_{N_1})_{\text{POCl}_3}}{(\eta_{N_1})_{\text{YAG}}} \eta_{d, \text{YAG}} = 0.04$$

The estimated long pulse performance of the Nd:POCl₃ liquid laser is shown in Figure 2-3. This prediction agrees quite well with the GTE results on a similar diameter laser shown in Figure 19 of reference 7. The GTE results do show a lamp saturation effect at higher powers. Nevertheless, we can confidently predict 50 J long pulse output at close to 3 percent overall efficiency.

2.3 Q-Switched Operation of the Nd:POCl₃ Laser

Q-switched performance of the Nd:POCl₃ laser will be determined by peak power damage considerations and nonlinear optical interactions such as stimulated Brillouin and Raman scattering in the laser liquid. Damage and nonlinear optic effects are dependent upon peak power density. The maximum peak output power is therefore dependent upon the cross sectional area of the laser cell.

Nonlinear optical interactions may limit the peak Q-switched power capabilities of an oscillator because they form an effective loss within the cavity. These effects may lengthen the Q-switched pulse length without seriously reducing pulse energy which may be useful for some applications.

Experiments have been performed at GTE Labs¹⁹ to determine the threshold power densities for SBS, SRS, and self-focusing. The experiments used a ruby laser to probe a 50-centimeter cell of POCl₃. No evidence of self-focusing was found for power densities in excess of 170 MW/cm². The threshold for SRS was found to be approximately 110 MW/cm². The threshold for SBS was found to be 35 MW/cm² for the ruby laser probe. However, SBS is

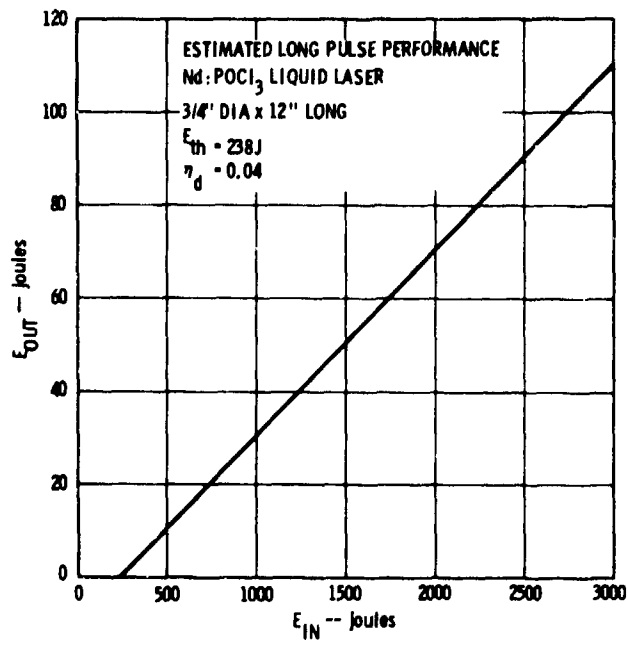


Figure 2-3. Estimated Long Pulse Performance of the Nd:POCl₃:ZrCl₄ Liquid Laser

dependent directly on the wavelength of the radiation.²⁰ Therefore, the threshold for SBS should be increased by the factor 1.06/0.69 to yield 54 MW/cm². Furthermore, the threshold for both²⁰ SRS and SBS depends inversely on the length of the active medium. The resultant thresholds, therefore, for stimulated Raman and Brillouin scattering are approximately 185 MW/cm² and 90 MW/cm², respectively, for a 30-centimeter cavity.

Table 2-2 gives the estimated values for onset of damage in various materials or onset of various nonlinear effects in POCl₃.

Table 2-2. Peak Power Densities for Damage of Various Materials and for Onset of Significant Nonlinear Effects in POCl₃ Cell 30 cm Long.

MATERIAL OR EFFECT	POWER DENSITY MW/cm ²	REFERENCE
LiNbO ₃	18	21
KD*P	100	16
Calcite	100	16
Quartz	1000	
Brillouin Scattering	90	
Raman Scattering	185	

If we eliminate LiNbO₃ from consideration as a Q-switch material, we see that we should be able to operate the Q-switched Nd:POCl₃ laser at least up to power densities of 90 MW/cm². For a 3/4-inch diameter laser cell with 2.84 cm² of area a minimum of 10 J of peak Q-switched energy should be obtained with 45 nsec pulse width.

3. FLOWING LIQUID LASER DESIGN

3.1 Laser Cell Design

A transverse flow configuration was chosen. The motivation for this approach was the rapid heat removal from the laser region which can be obtained even at moderate flow velocities with low pressure head loss. Transverse flow devices should be extendable to extremely high repetition rates and high average power operation, before pressure losses in the laser cell become significant.

The transverse flow cell design is shown in cross section in Figure 3.1. Laser liquid enters at the bottom, goes through a row of straightening fins and into the laser cell. The laser cell has sharp edged nozzles at the inlet and outlet and has a cylindrical configuration, 3/4 inch in diameter and 12 inches long. This design has a very small light leakage path from the optical pump cavity, and the sharp edge nozzles cause flow separation that induces turbulence and promotes mixing and liquid uniformity.

The pump cavity is of the close coupled type with a wedge condenser and a cylindrical condensing lens concentrating pump light into the laser cell. The arc lamp is cooled with axial water flow in a concentric annulus around the lamp.

Materials utilized in the design are not corroded by the laser liquid. The main structure is made of pure nickel 200. The pump cavity window is made of fused quartz. "O" rings for sealing are made of teflon with rubber central cores.

The head loss⁽²²⁾ through the liquid laser cell was calculated step by step through each of the transitions from the inlet pipe to the outlet pipe. The calculated head loss was 2 feet of liquid at 20 gal/min flow rate. As a function of flow rate, Q , in gal/min the cell head loss, h_c , in feet was

$$h_c = 0.005Q^2 \quad (3-1)$$

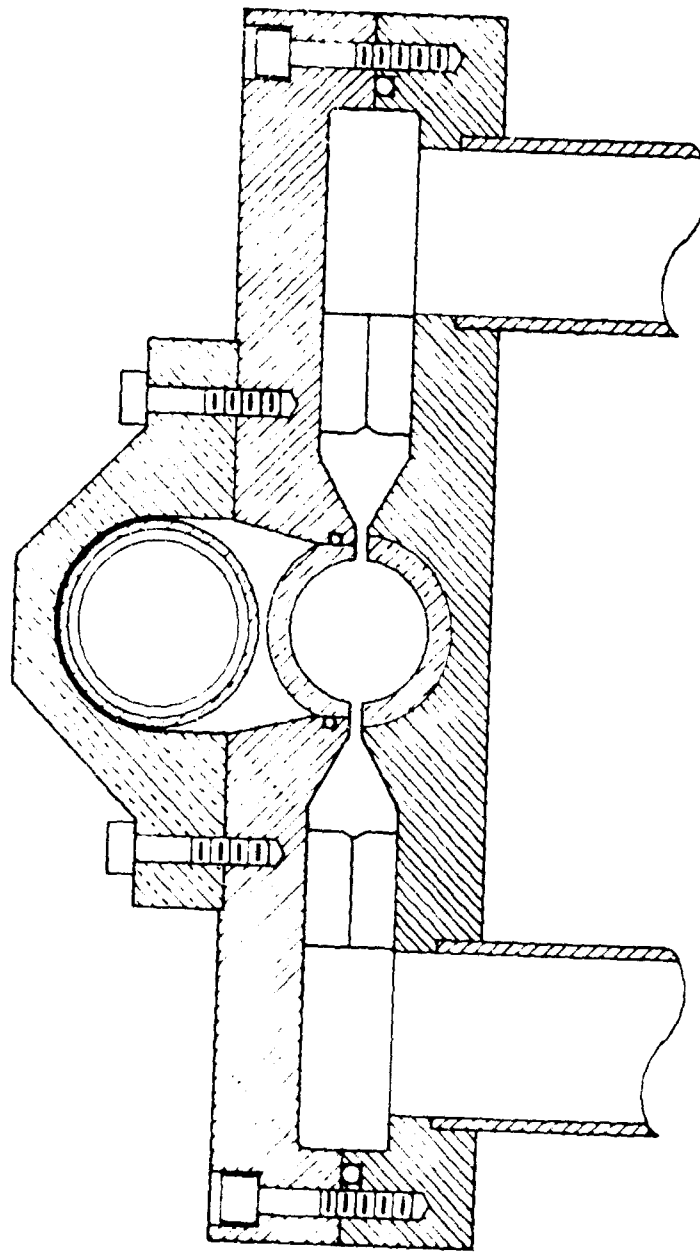


Figure 3-1. Cross Section of Liquid Laser Cell

The transverse flow cell design was tested with a hydrodynamic model prior to fabrication to establish the interferometric quality of the cell design and to measure the head loss. The model is shown in Figure 3-2.

A Twyman/Green interferometer was constructed to measure the optical path distortion in the liquid cell during flow. The interferometer with the liquid cell in position is shown in Figure 3-3. The beam from a He-Ne laser is expanded in diameter, split in a solid cube beam splitter, and makes a double transverse of each of the legs of the interferometer. One of the interferometer legs contains the liquid cell. The two beams recombine at the beam splitter and the interference pattern is photographed with a camera.

Water-ethylene glycol mixture with a Reynolds number equivalent to POCl_3 was circulated through the cell. Three centrifugal pumps were used to provide continuously variable flow up to 20 gal/min. The pump arrangement is shown in Figure 3-4. Measured head loss at 20 gal/min flow was 1.6 feet which was very close to the calculated 2 feet.

Interference fringe photographs for various flow rates are shown in Figure 3-5. No significant distortion was found at any flow rate. The fringe visibility was worse at higher flow rates due to fringe motion. This was due to greater mechanical vibration and temperature variations in the liquid and air paths during flow. Optical path distortion is our concern and average path change is of little importance.

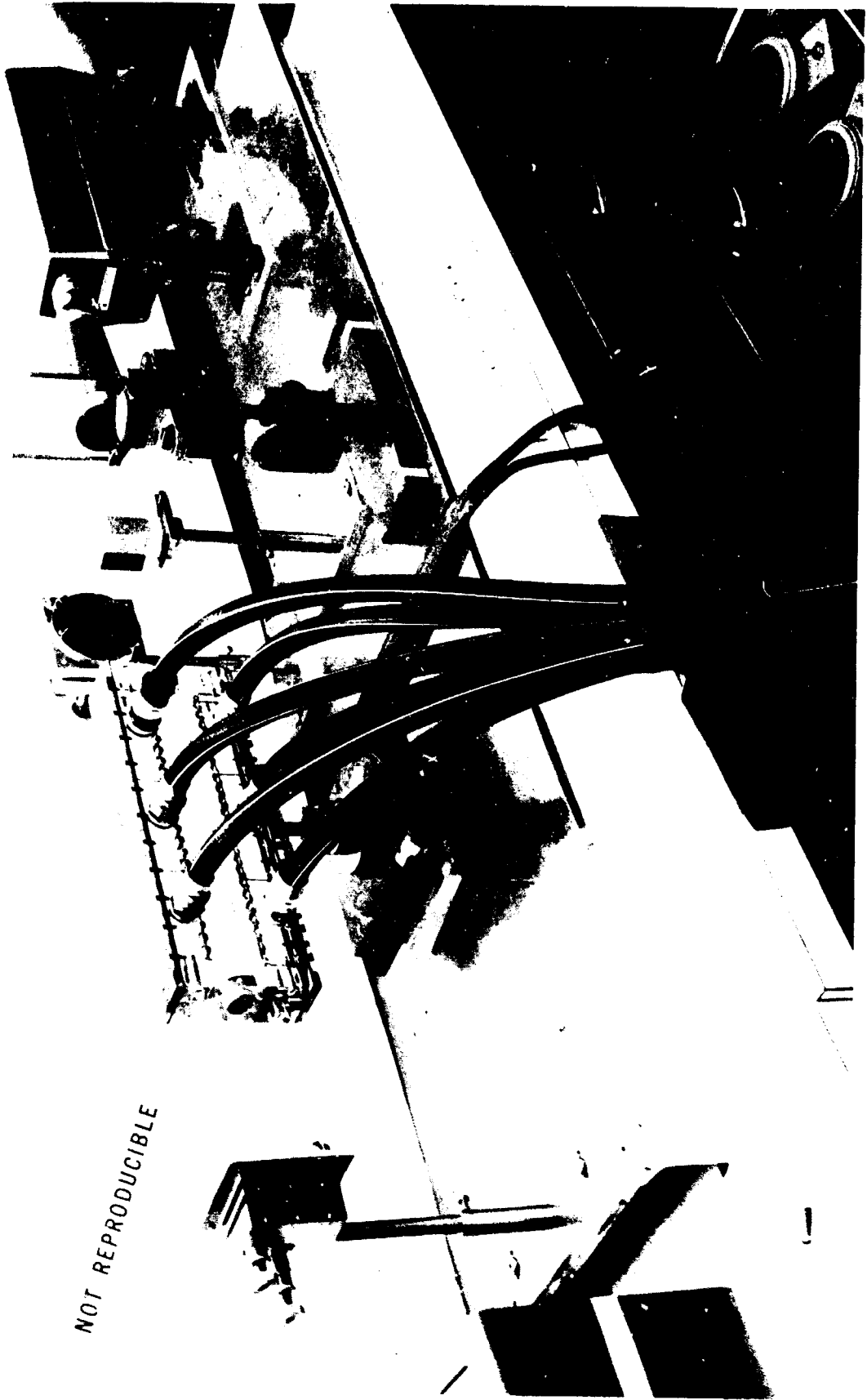
These results were very encouraging and though there was no pumping heat load they indicate that the cell design produces interferometer optical quality liquid in the cell.

3.2 Liquid Laser Circulation

The liquid laser cavity and cooling system have been designed totally of nickel which is not corroded by the laser liquid. Teflon which is similarly not corroded has been used for seals and for some valves and pipes. A flow diagram is shown in Figure 3-6. The laser liquid is circulated through the laser and then a heat exchanger by a centrifugal pump. The liquid flow



Figure 3-2. Hydrodynamic Model of the Transverse Flow Liquid Laser Cell



NOT REPRODUCIBLE

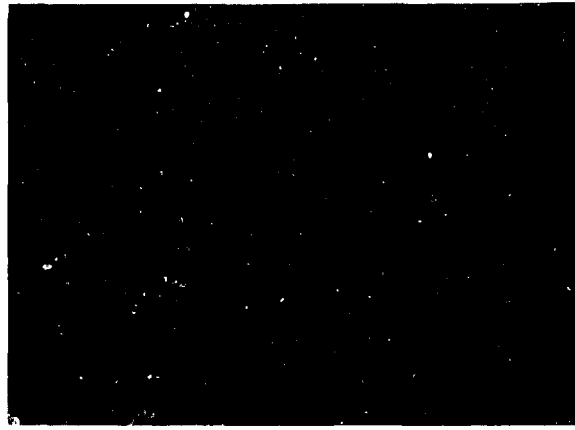
Figure 3-3. Twyman/Green Interferometer for Measuring Optical Distortion in the Laser Liquid Cell.



Figure 3-4. Liquid Pumping Arrangement.



a. No Flow



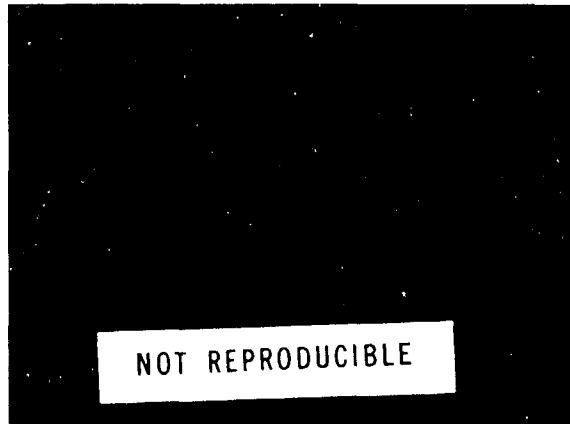
b. 10 gal/min.



c. 13 gal/min.



d. 15 gal/min.



e. 20 gal/min.

Figure 3-5. Twyman/Green Interferometer Fringes Through Model Liquid Laser with Flowing Water - Ethylene Glycol Mixture Matching Reynolds Number of POCl_3

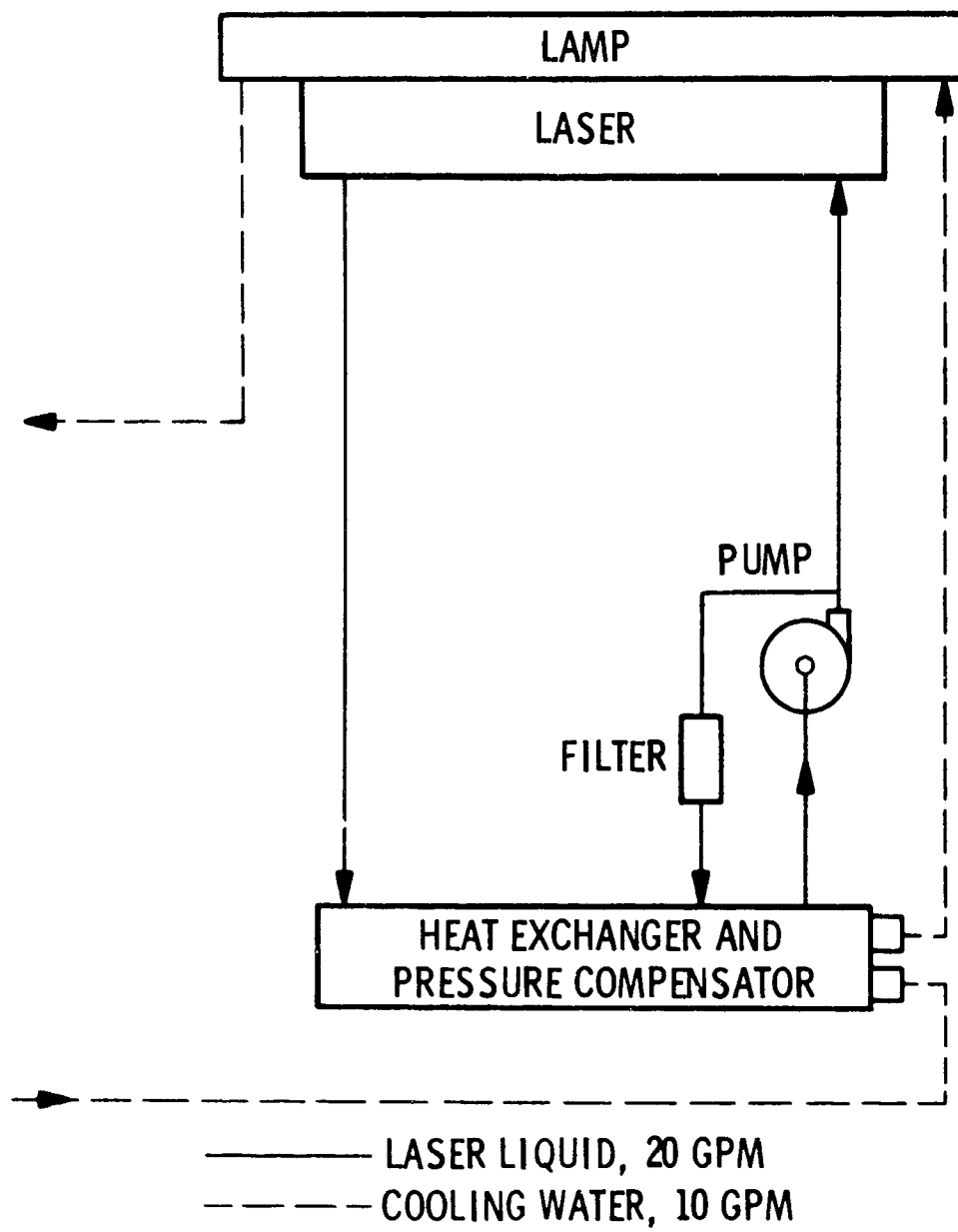


Figure 3-6. Flow Diagram for the Liquid Laser.

rate is approximately 20 gal/min. This rate ensures new liquid every pulse at 10 pps rate. A small portion of the liquid is continuously bypassed and filtered. A spring loaded piston is provided on the heat exchanger to maintain a positive pressure in the system and to compensate for liquid volume changes. Cooling water flows through the tube side of a shell and tube heat exchanger and then around the pump lamp.

The completed liquid laser system is shown in Figures 3-7 and 3-8. Liquid flows from the centrifugal pump into the bottom of the laser cell. It then flows out the top of the cell through the heat exchanger and back to the inlet of the pump.

All tubing was 1.37" I.D. x 1.50" O.D. nickel 200. The pump selected was modified from a 1 1/4" P.T. inlet and 1" P.T. outlet to mate with the 1.50" O.D. nickel tubing. One joint in each run of tubing was made using nickel flanges, teflon covered silicon rubber "O" ring and "Vee" band clamps. This allowed freedom of rotation about one axis during assembly. The second joint in each run of tubing was made with teflon tubing of 1.50" I.D. x .040 wall thickness. A machined teflon collar was fabricated with the same wall thickness as the nickel pipe and inserted before sliding the teflon tubing over the nickel tubing ends. The teflon tubing was clamped in place using ordinary hose clamps lined with neoprene for equal distribution of force on the teflon. No significant problem was encountered with either type of joint although the "V" band connected joints are much simpler to assemble and will withstand considerably higher internal pressure.

The total fluid system was designed to produce turbulent flow in all parts of the system, including the interconnecting pipe. The critical lower value for transition from laminar or streamline flow to turbulent flow is at a Reynolds number of approximately 2000, where the dimensionless Reynolds number²² is as follows:

$$N_R = \frac{DV\rho}{\mu}$$

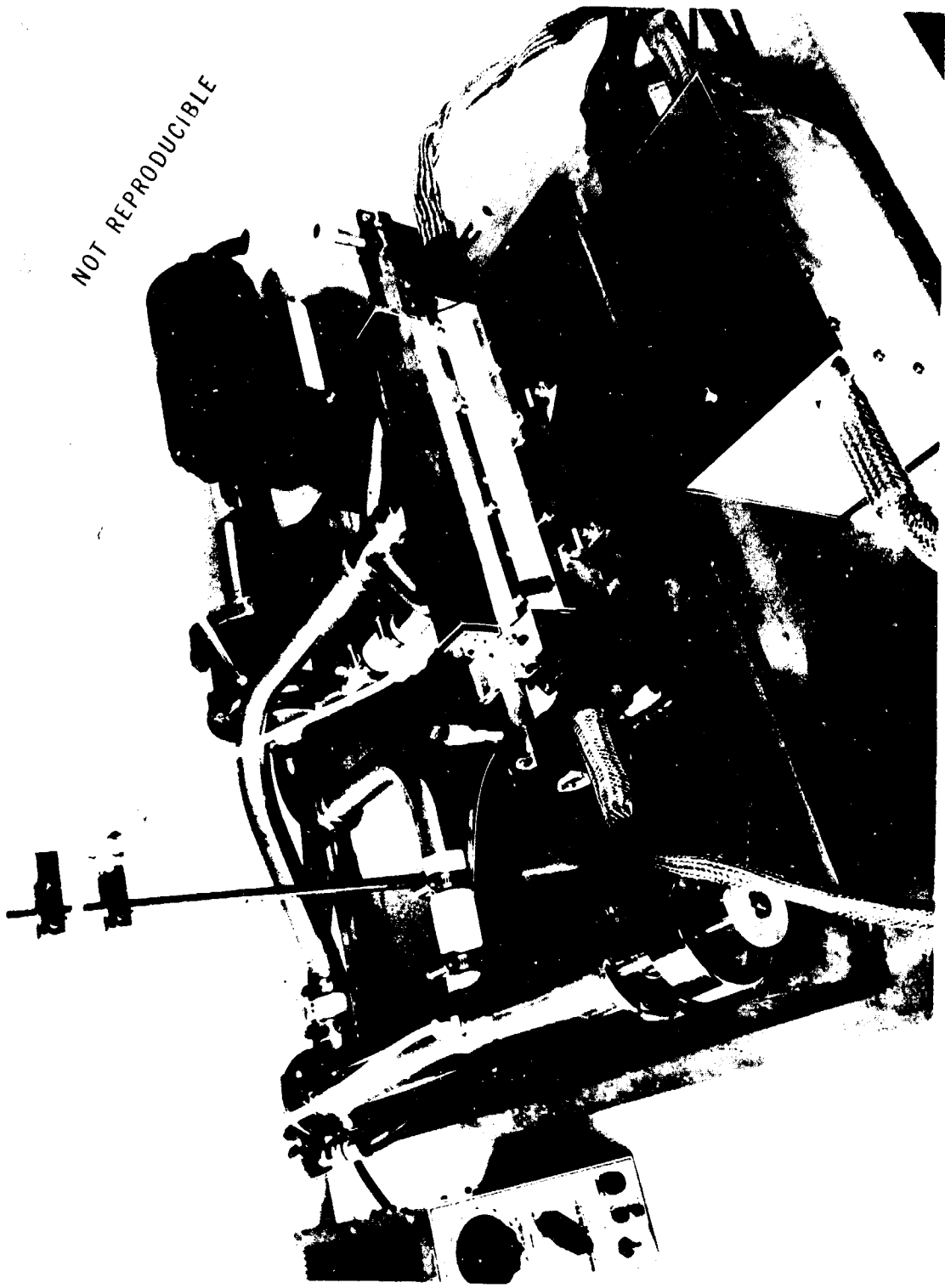


Figure 3-7. Liquid Laser Circulation System.

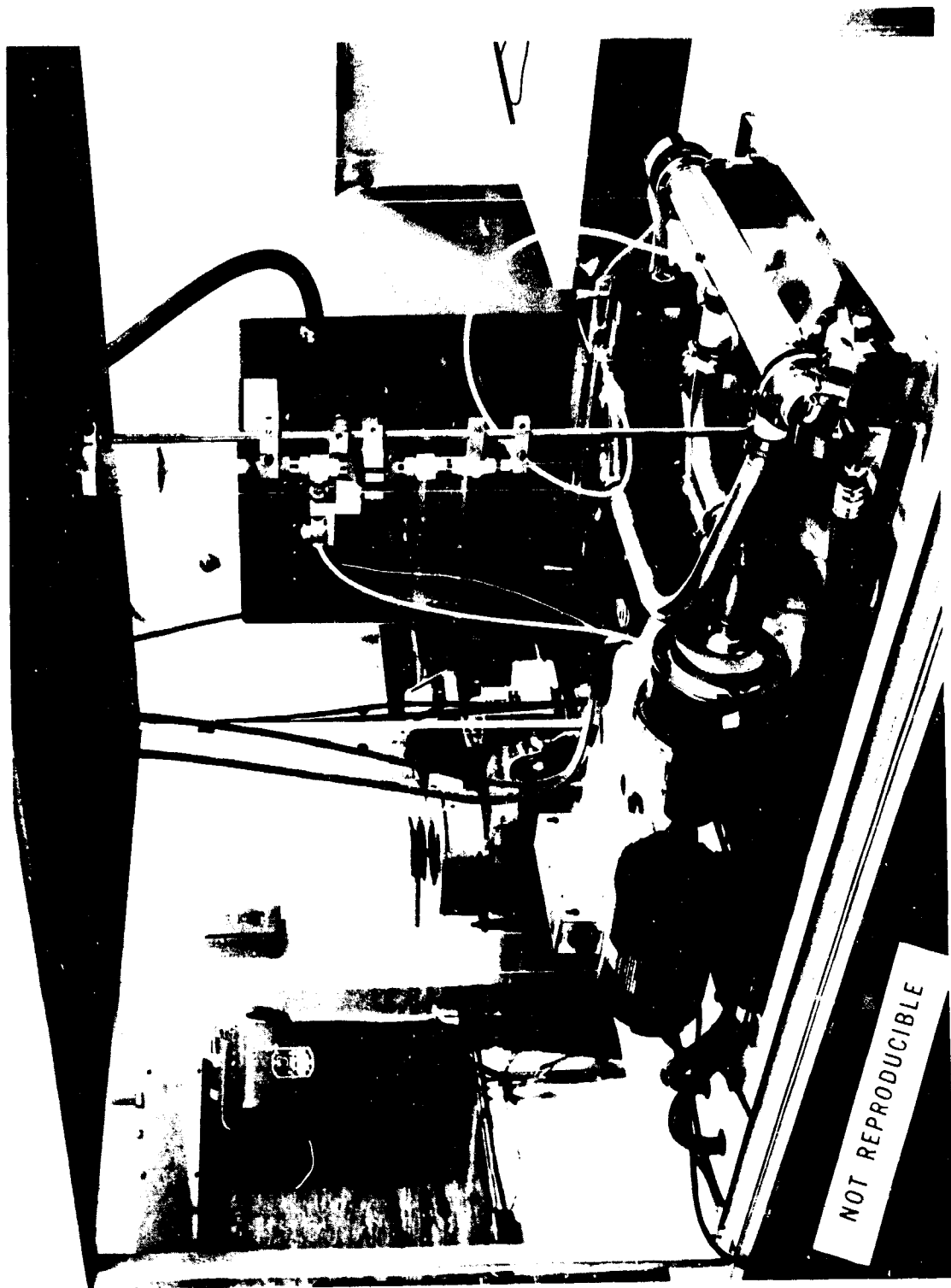


Figure 3-8. Liquid Laser System.

and

- D = inside diameter of conduit in feet
- V = average velocity in feet per second
- ρ = density, lbs. fluid per cubic foot
- μ = absolute viscosity of fluid lb/sec feet

The Reynolds number in the piping used for this system is 15,400 at a flow rate of 20 gpm through 1.37" I.D. pipe. This is well into the turbulent flow range.

The entire fluid flow system was designed for minimum pressure drop and high velocity flow rates. The interconnecting tubing was sized to limit flow velocities to 6 feet per second which is a commonly accepted fluids engineering value resulting in reasonable pressure losses and low acoustic levels.

The head loss in the piping was calculated to be 1.54 feet of liquid at 20 gal/min flow rate. As a function of flow rate, Q, in gal/min the piping head loss, h_p , in feet was:

$$h_p = 0.0039Q^2 \quad (3-3)$$

3.2.1 Heat Exchanger

The heat exchanger was designed around the following requirements:

1. Dissipate 3 kW of heat from the laser liquid.
2. Cooling water flow rate 10 gal/min with 60°F inlet water temperature.
3. Laser liquid flow 20 gal/min.
4. Minimum pressure drop on the laser liquid side.
5. Laser liquid temperature to be less than 75°F.
6. Minimum volume on laser liquid side of heat exchanger.
7. Maximum exclusion of water from mixing with the laser liquid.
8. Provisions for system volume changes due to thermal expansion of the laser liquid.

A shell and tube heat exchanger was chosen as the best solution to the problem because of the proven design technique, the availability of nickel tubing and pipe and the relative ease of construction. The actual design has six baffled shell passes and two tube passes. The laser liquid was routed through the shell side since it was the more viscous and had the more severe limitation on pressure drop²².

The design of a heat exchanger is an iterative process whereby some log mean temperature difference, approximate surface area, and overall heat transfer coefficient are assumed and the resultant configuration checked to see if it agrees with the assumptions. The heat transfer coefficient is based on a series of resistances consisting of the outer film coefficient on the tube, the tube material resistance, and the inner film coefficient. In this design the fairly high conductance of nickel results in the inside and outside film coefficients being the factors of prime importance.

A typical film coefficient for water inside clean tubes would be based on the following formula²³.

$$h_i = 160 (1 + .012 T_f) \frac{V_s^{.8}}{D_i^2} \quad (3-4)$$

h_i = internal tube heat transfer coef. in BTU/hr/ft²/°F

$$t_f = \frac{t + t_w}{2} \text{ and}$$

t = bulk liquid temp., °F

t_w = wall temp., °F

V_s = average velocity, f.p.s.

D_i = inside tube dia., inches

This is correct if the Reynolds number is greater than 7000, the velocity and tube diameter was selected to meet or exceed this criteria. The length/diameter ratio of the tubes was such that they could be considered long tubes using velocities of 6 f.p.s. and 1/4" nominal tubing with .032 wall gives values for h_i between 1500 - 2000 BTU/hr/ft²/°F.

A typical film coefficient²² for the flow of liquids (POCl_3) outside staggered tubes with Reynolds numbers greater than 2000 is given by:

$$h_o = \frac{K_f}{D_o} .33 \frac{(C_p \mu)^{1/3}}{k} \left(\frac{D_o G_{\max}}{\mu_f} \right)^{.6} \quad (3-5)$$

h_o = external tube coefficient BTU/hr/ft²/°F

where K_f = thermal conductivity of fluid,

(this was calculated as $.100 \frac{\text{BTU/ft}^2/\text{°F}}{\text{hr ft}}$)

D_o = outside diameter of tube, feet

C_p = specific heat BTU/lb °F
(calculated from Kopp's rule as $.244 \text{ BTU/lb. °F}$)

μ = absolute viscosity of fluid lb/sec. ft.
($\mu = .000672 \times$ viscosity in centipoises)
(5.4 centipoises for laser liquid)

G_{\max} = mass velocity, lb/sec. ft² of cross section

μ_f = absolute viscosity of fluid at the wall or film.

Typical values for the tube sizes and spacings selected gives value of h_o of approximately 1000. This was reduced by 30% to a value of 700 to account for leakage of some fluid by the baffles. The overall coefficient of heat transfer is then:

$$\text{Overall coefficient} = \frac{1}{(hA)_T} = \frac{1}{h_i A_i} + \frac{1}{R_m} + \frac{1}{h_o A_o} \quad (3-6)$$

The overall coefficient was determined for an outside tube area of 1 ft² and using the formula²³:

$$Q = (UA) \Delta T$$

where Q = total heat flux, BTU/hr

UA = overall coefficient x area = BTU/hr °F

ΔT = temperature difference between laser liquid and cooling water, °F.

The total heat flux was known (3000 watts) and ΔT was to be some value between 10-15°F, the quantity UA could be adjusted by increasing the surface area, in this case making the water flow tubes longer by increasing the heat exchanger length. The end result was a surface area of slightly over 2.1 ft² on the outside of the tubes, an overall U of 500 resulting in a ΔT between laser liquid and cooling water of 10°F. The overall dimensions of the heat exchanger were approximately 3" in diameter by 18" long.

The tube bundle and the pressure compensation piston for the final heat exchanger are shown in Figure 3-9. The completely assembled heat exchanger is visible in Figures 3-7, 3-8, and 3-9.

Pressure head loss through the shell side of the heat exchanger was calculated²² in a stepwise manner. The calculated head loss was 4.3 feet of liquid at a flow rate of 20 gal/min. As a function of flow rate, Q, in gal/min, the head loss, h_e, in ft. was:

$$h_e = 0.0108 Q^2 \quad (3-7)$$

3.2.2 Pump

A commercial corrosion resistant nickel pump manufactured by the R. S. Corcoran Co. was modified for use with the laser liquid. A Crane face seal was used to seal the pump shaft. This seal was flooded with mercury to prevent water vapor from reaching laser liquid at the seal. A

NOT REPRODUCIBLE

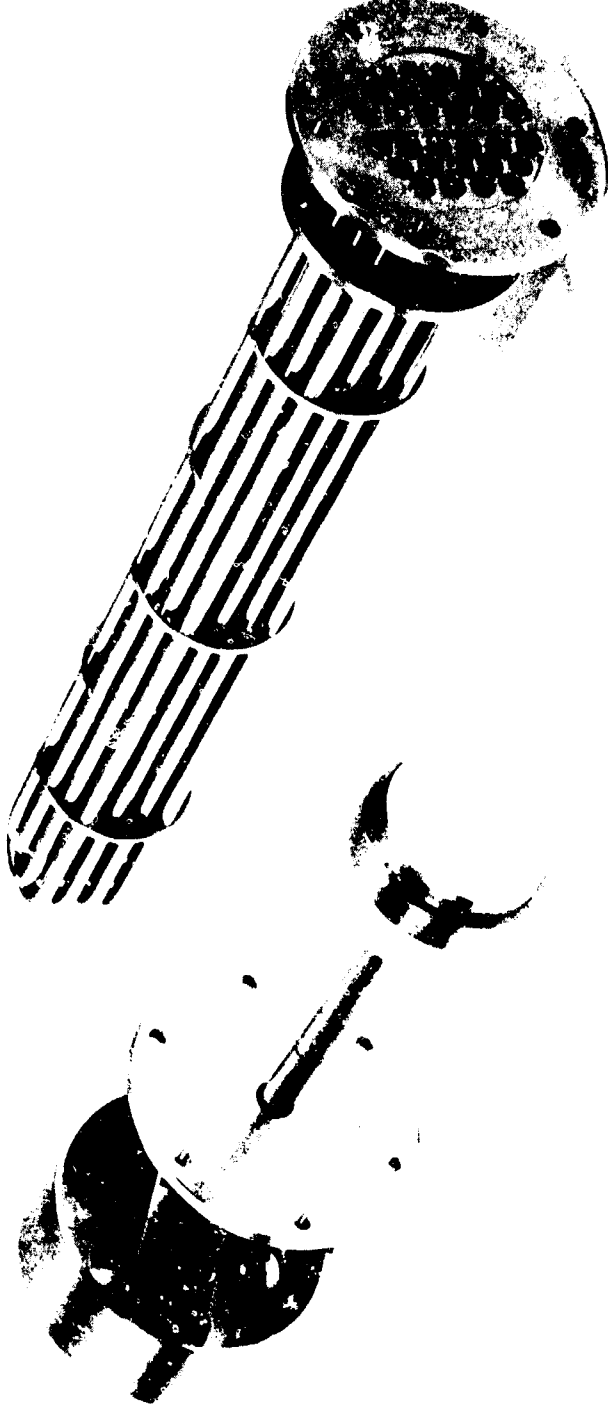


Figure 3-9. Liquid Laser Heat Exchanger Core and Pressure Compensation Piston.

69120453

schematic cross section of the seal is shown in Figure 3-10.

A nickel ring was welded inside the pump to form a cavity in the high pressure area between the seal and the impeller. Liquid was continuously drawn from this cavity into the filter. Any particles produced by wear at the face seal should be immediately deposited in the filter.

One rubbing face of the seal was made of alumina. This alumina was bonded into the nickel housing using an epoxy which is quite resistant to the liquid (EpoxyLite #5403). The second rubbing face is of either carbon or glass filled teflon. A spring-loaded conical piece of teflon mates with the back of this material to seal to the pump shaft. A housing surrounding the seal assembly provides the chamber to hold the mercury. An "O" ring seal holds the mercury. A chamber filled with oil provides lubrication for this seal. The "O" rings are made of viton which is not affected by laser liquid vapor.

The pump was driven by a one horsepower Minarik speed control motor. The pump characteristics as a function of motor control setting in percent are shown in Figure 3-11. Also shown is the system load line which is represented by the sum of the head losses in equations 3-1, 3-3 and 3-7:

$$h_{\text{total}} = 0.02 Q^2 \quad (3-8)$$

The system will flow almost 40 gal/min through the laser cell at the maximum pump speed setting. This corresponds to new liquid in the cell 29 times per second.

3.3 Power Supply

The power supply for the liquid laser is shown in Figure 3-12. Single phase 480 volt, 60 Hz power enters a contactor. This power is applied to a variable transformer which controls the voltage applied to a "step up" transformer. SCR's are provided in the primary circuit to restrict the recharging time and prevent continuous arc over in the laser flash lamps.

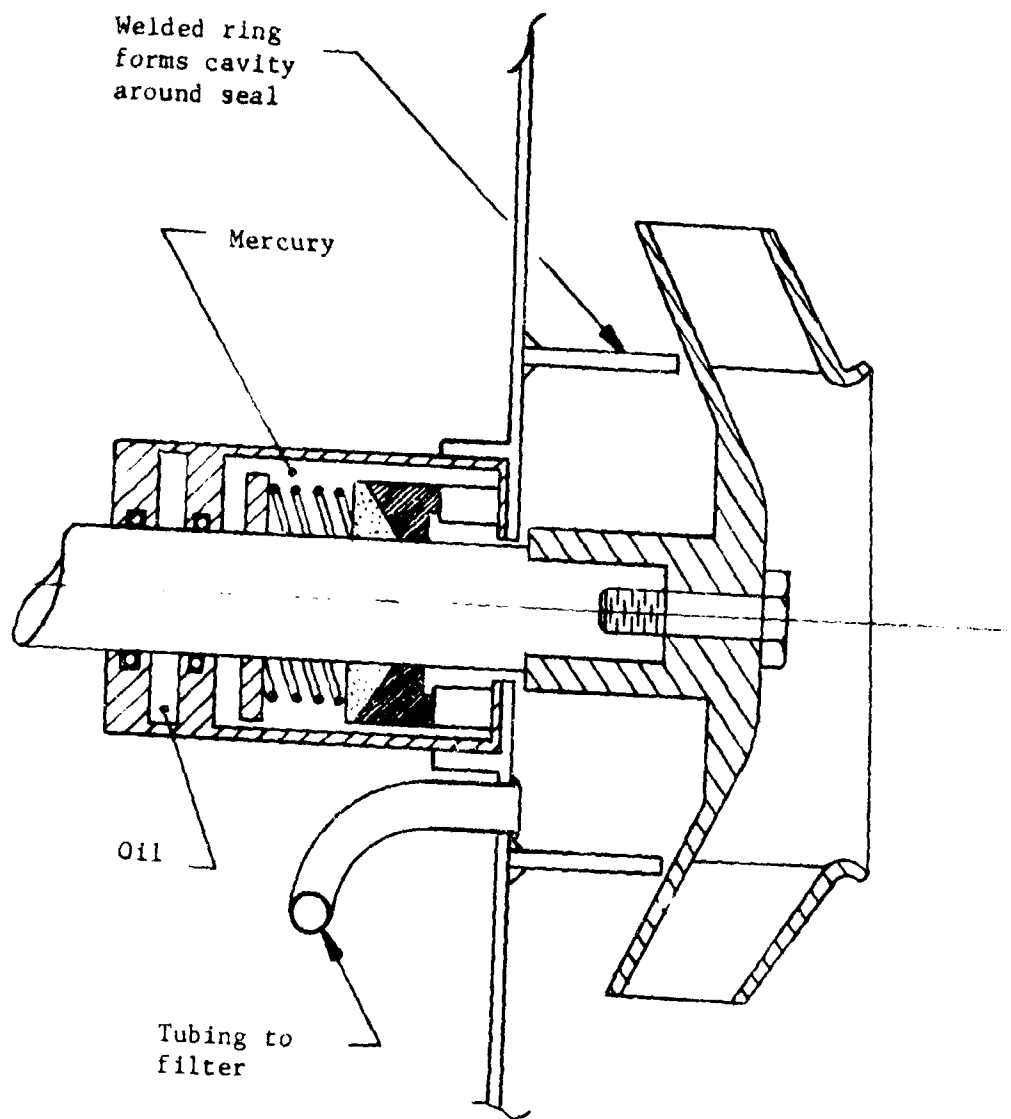


Figure 3-10. Face Seal Schematic for
Liquid Laser Pump.

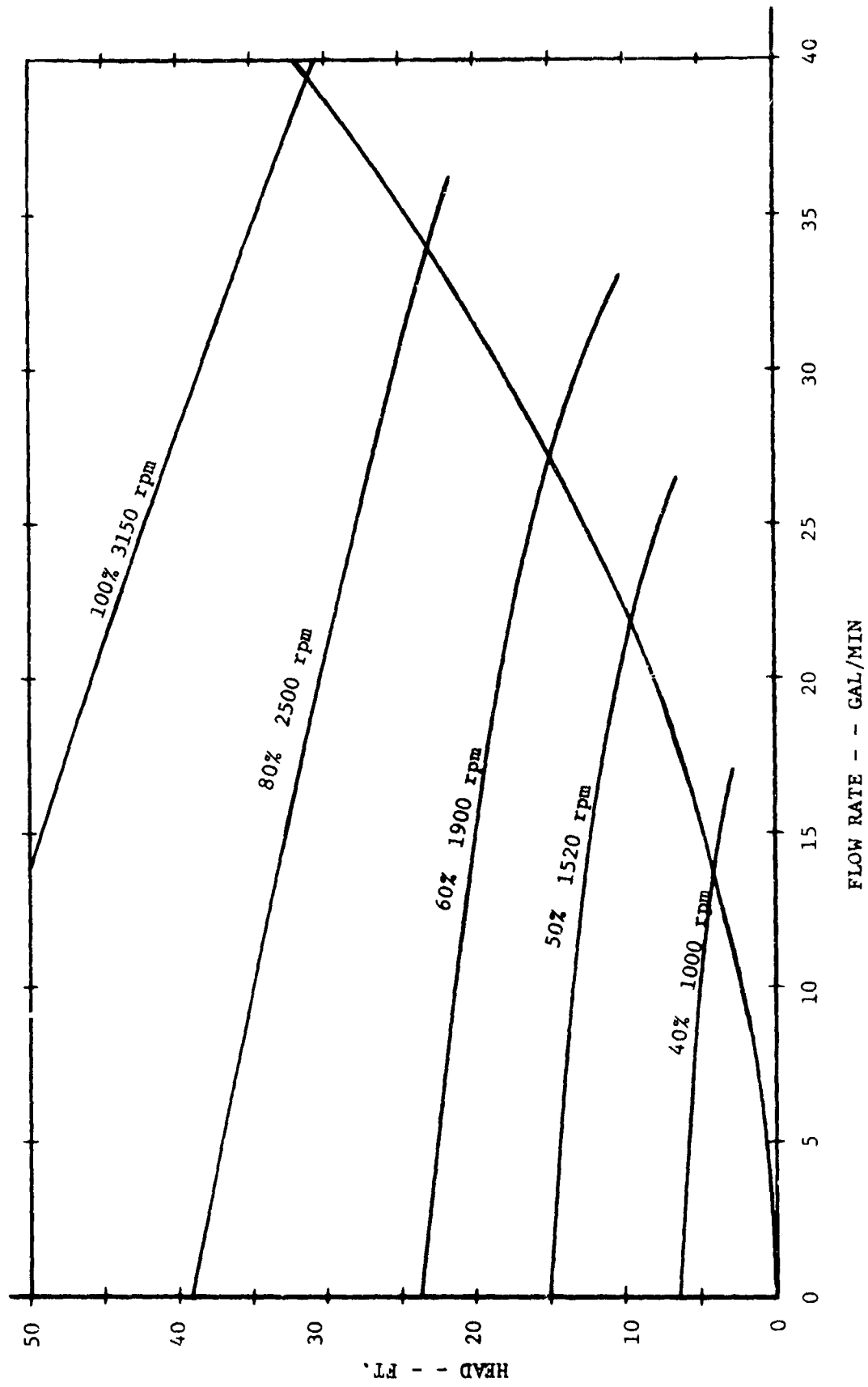
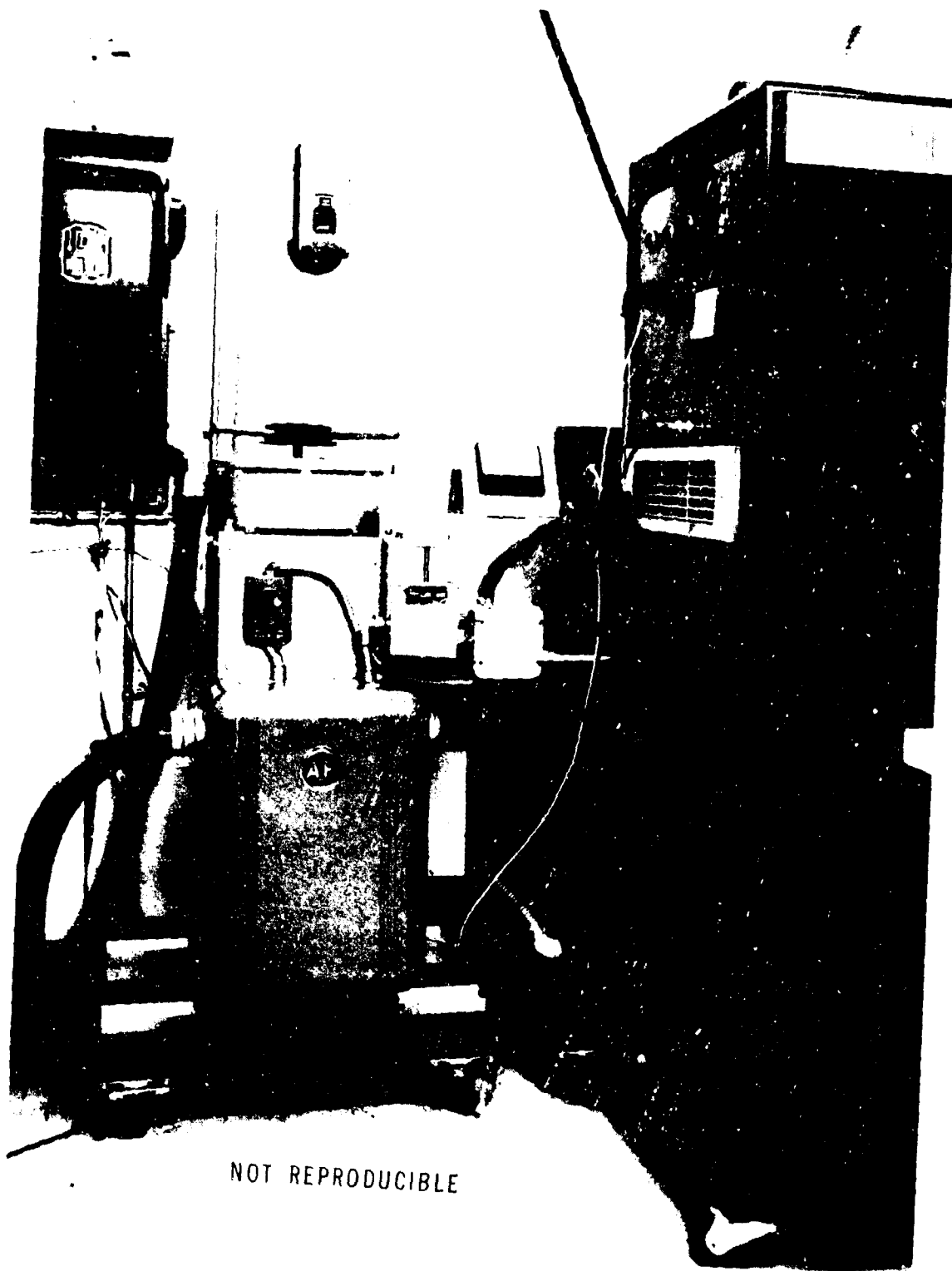


Figure 3-11. Pump Characteristics and System Load Line for Liquid Laser System.



NOT REPRODUCIBLE

Figure 3-12. Liquid Laser Power Supply.

The output from the secondary of the transformer is rectified and used to charge the capacitor bank.

The power supply is fully safety interlocked for cooling water flow and the cabinet doors.

A schematic of the lamp firing circuit is shown in Figure 3-13. The charged capacitor bank, C, is discharged through the laser pump lamp by breaking down the lamp with a high voltage pulse from the series trigger transformer. The inductance and capacitance are chosen to give the desired pump light pulse length and to provide a near critically damped discharge of the capacitors into the flash lamp²³. The network for the liquid laser was designed to give a pump lamp pulse 300 μ sec long.

3.4 Q-Switching

Two mechanical Q-switching arrangements were designed and fabricated for the liquid laser. These are shown in Figure 3-14. The arrangement shown in Figure 3-14a utilizes a simple rotating Porro prism²⁵. This rotating Porro prism Q-switch is shown in Figure 3-15. A 24,000 rpm synchronous motor powers the carefully balanced prism assembly through a flexible coupling. A light and photocell combination provides a suitable lead time fire signal from a stripe painted on the rotor.

Figure 3-14b shows the second mechanical Q-switching arrangement. This utilizes a rotating Brewster's angle totally internally reflecting prism and a stationary Porro prism. Figure 3-16 shows the assembled rotating Brewster's angle prism.

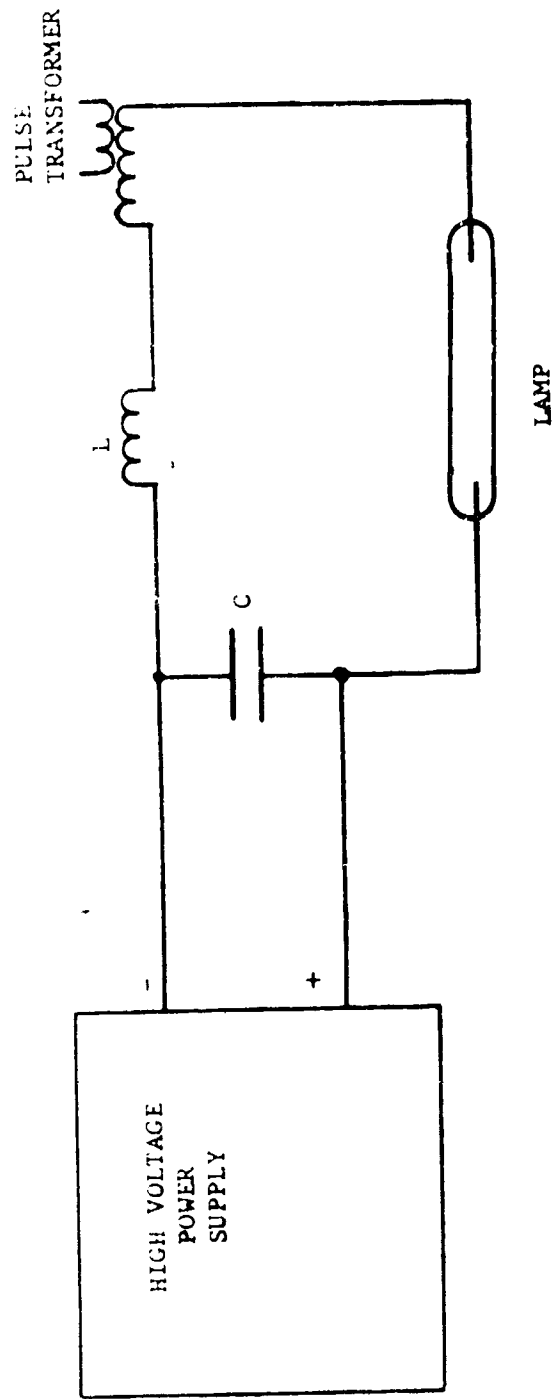


Figure 3-13. Liquid Laser Lamp Firing Circuit.

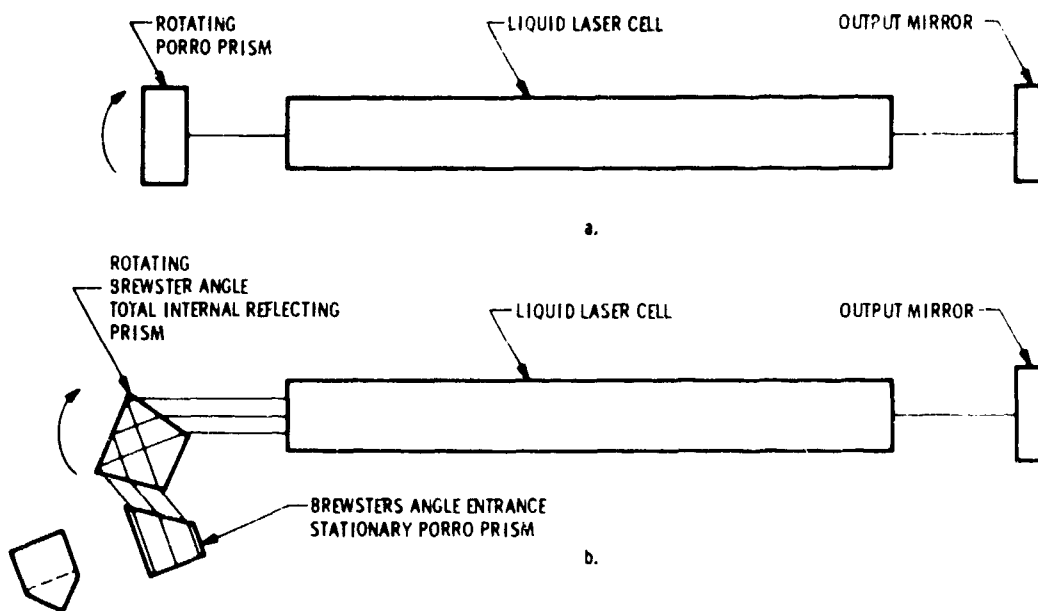


Figure 3-14. Mechanical Q-Switching Arrangements for the Liquid Laser.

NOT REPRODUCIBLE



Figure 3-15. Rotating Porro Prism Mechanical Q-Switch.

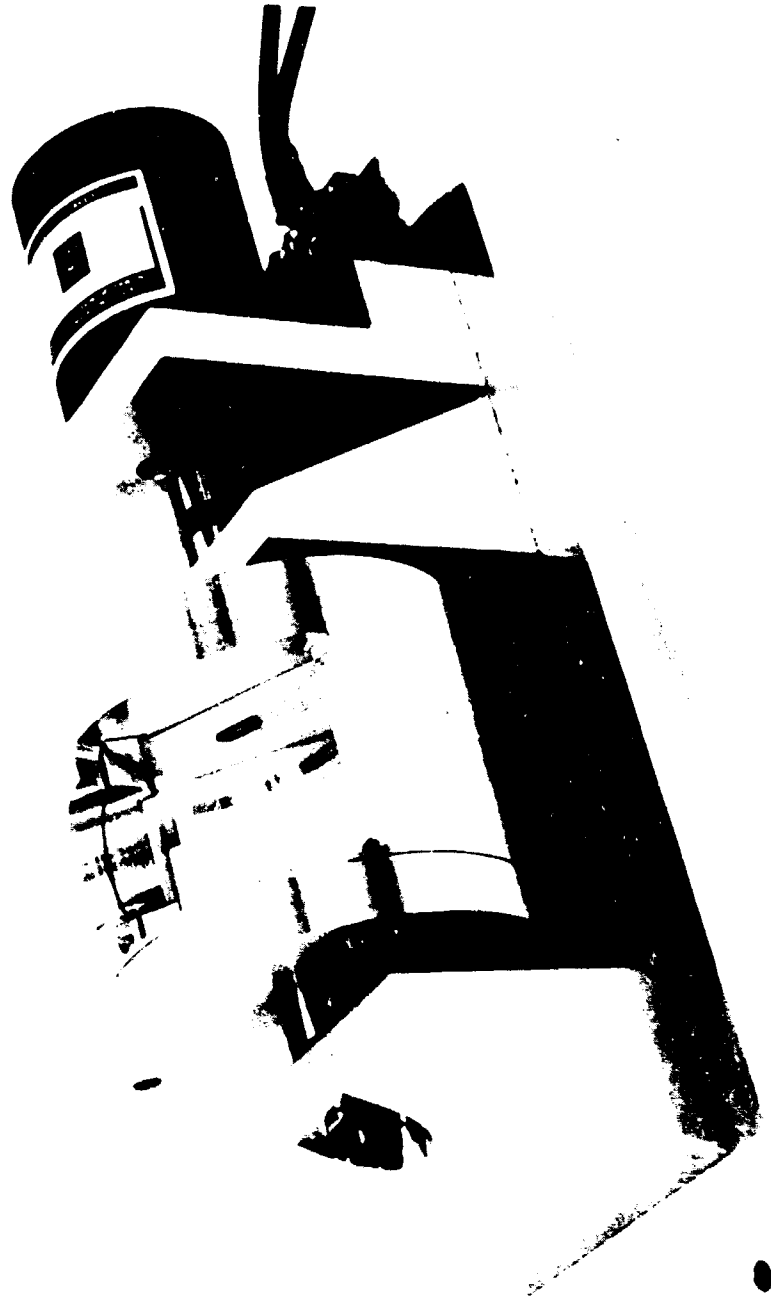


Figure 3-16. Rotating Brewster's Angle Total Internal Reflecting Prism Mechanical Q-Switch.

NOT REPRODUCIBLE

4. ASSEMBLY AND FILLING OF THE LIQUID LASER

4.1 Assembly Procedure

Assembly of the laser cell is shown in Figure 4-1. Successful achievement of this assembly proved to be a difficult problem. The longitudinal teflon "O" rings which sealed the side window of the cell would not seal properly. The major problem was at the ends of the seals where a collar and plug arrangement mated with the rubber-filled teflon tubing "O" rings. A series of assembly attempts were made with increasing preload on the teflon seals. The liquid leakage continued to decrease and was essentially eliminated when the quartz window began to break due to the seal pressure. Calculations showed the quartz stress was approximately 1000 psi tension at the point where the break was initiating. The laser cell could be successfully assembled in a leak free condition and after several hours the quartz would break. This of course is what is expected from a brittle material subjected to sufficient stress for crack nucleation and growth.

Altogether, the system was assembled over 25 times with either leaks or breaking of the quartz window. Successful assembly appeared impossible. Materials testing had continued throughout this period, however, and a material with good resistance to the laser liquid was found which could be used as an auxiliary sealant. This was Dow Corning Fluorsilicone Silastic 733 RTV. The material is very similar to silicone rubber in appearance. It does not seem to affect the laser liquid even after long exposure. It does slowly break up if completely exposed to the POCl_3 laser liquid but with limited exposed material in a seal seems to last for long periods.

Use of a very small portion of the 733 sealant at the critical points solved the leakage problem and allowed reductions in the seal pressures which solved the window breakage problem. The laser liquid cell was then successfully assembled.



NOT REPRODUCIBLE

Figure 4-1. Assembly of the Transverse Flow Liquid Laser Cell.

The laser cell side window was designed to have support so that it would withstand the fluid pressure at high flow rates. This support was provided by three glass spacers on the glass lamp flow tube. These spacers transferred the force from the laser cell window to the flow tube. The flow tube in turn was supported by adjustable spacers in the back reflector of the pump cavity. Each of these spacers was adjusted during the assembly.

4.2 Filling Procedure

Before assembly each of the metal flow system parts was chemically cleaned. The assembled system was therefore in a clean condition before filling.

All water must be removed from the system before filling. This was attempted by purging the system for twenty-four hours with a flow of dry nitrogen before filling with the $\text{Nd:POCl}_3\text{:ZrCl}_4$ laser liquid.

The laser liquid was manufactured by the Chemical and Metallurgical Division of GTE Sylvania, Towanda, Pa., where it is commercially available. The liquid was supplied in sealed bottles.

The system was filled by applying dry nitrogen pressure to a bottle and forcing the liquid up through a glass pipe which terminated at the bottom of the bottle and was connected by teflon tubing to the system. With this technique, the liquid was never exposed to atmospheric water vapor. The bottle was enclosed in a stainless steel container for safety.

Once the system was filled, it was necessary to remove any gas that was trapped in the system. The pump was slowly rotated to flow the fluid and pick up the gas as bubbles in the liquid. The filter system proved to be an effective gas elimination system. Gas would collect at the pump outlet to the filter and at some low pressure teflon tubing locations.

This gas was then bled from the top of the system as additional liquid was introduced from the filling bottle. During this operation the liquid was allowed to rise in temperature up to about 120°F by the energy input from the pump. The higher temperature facilitated removal of the gas by reducing the gas solubility in the liquid. After about an hour the liquid became completely gas free.

When the system is first filled the laser cell is very clear and transparent. As the gas becomes entrapped in the liquid the scattering loss becomes so high that the cell is essentially opaque. After the gas is removed from the liquid, the liquid again becomes clear and transparent.

5. EXPERIMENTAL RESULTS

5.1 First Series of Experiments

The system is shown in Figure 3-1 and is described in Section 4.2. The one exception in this first filling was the pump shaft seal. A glass filled teflon rotating element and a stationary alumina face seal was used without the mercury surrounding the outside of the seal.

After filling with liquid, the pump was started and the degassing operation begun. The face seal started to leak after about 30 minutes of pump operation. The liquid was then drained from the system, the pump removed from the system and disassembled. The face seal was found to be covered with particles precipitated from the laser liquid. These particles had abraded the seal badly and caused the leak.

The pump was cleaned and reassembled with a carbon and alumina face seal with mercury wetting the outside of the seal. The pump was heated in an oven for 2 hours at 200^oF to dry it out before reassembly to the system. Upon reassembly and filling, the pump was found to have a small leak from its main "O" ring seal.

The pump was again disassembled and found to be coated with a white precipitate wherever it had contacted the liquid. The pump was cleaned again and heated in the oven for 16 hours at 200^oF. The system was then reassembled and filled with no leaks.

Scattering in the liquid cell was quite bad compared to the original condition. It was decided that static lasing experiments should be run before flowing the liquid and possibly further increasing the scattering. The long pulse (300 μ sec) static liquid output energy versus input energy results are shown in Figure 5-1.

The laser liquid was then degassed by flowing for about one hour. A HeNe laser beam came through the flowing liquid very well. The scattering losses were moderate.

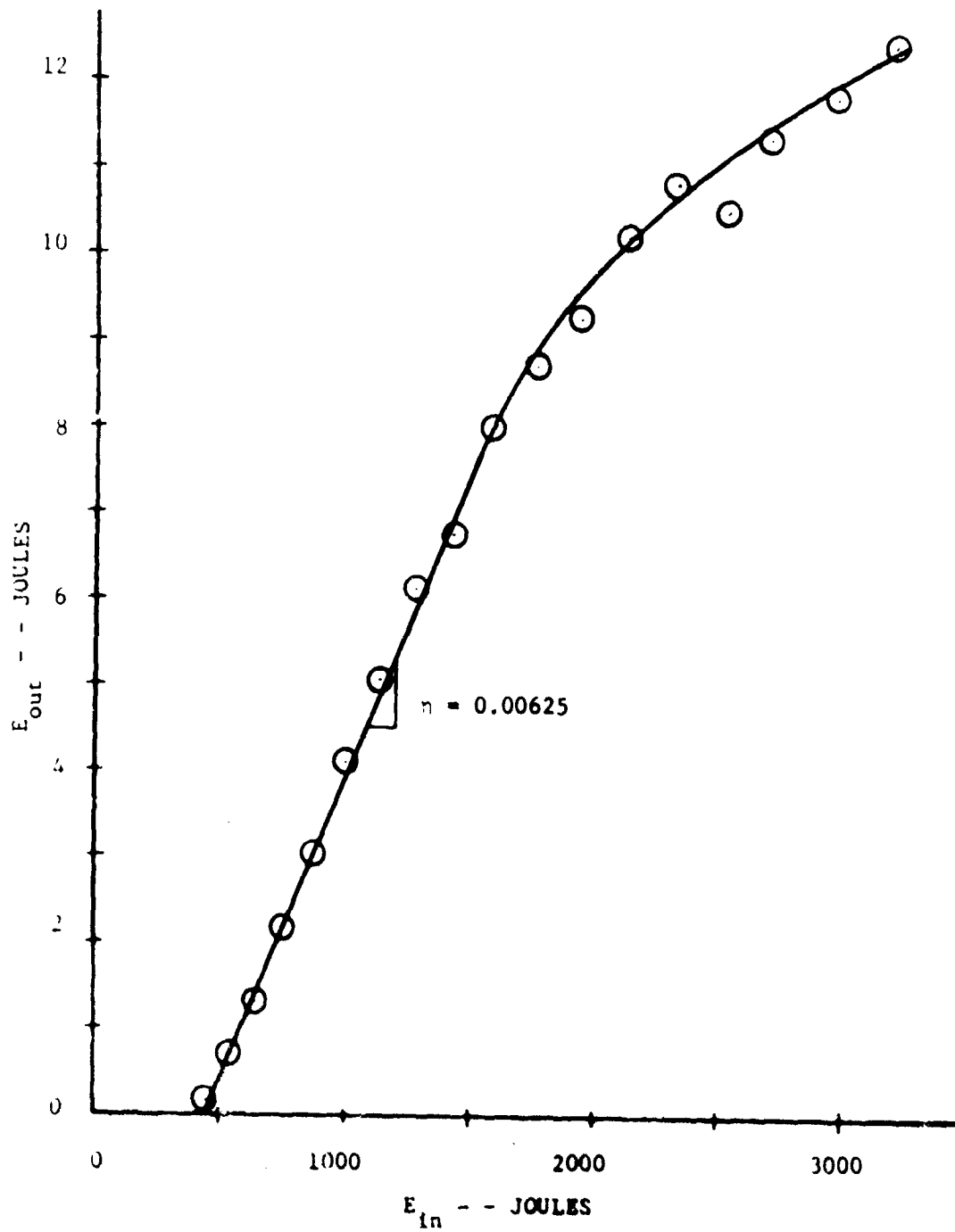


Figure 5-1. Long Pulse (300 usec) Static Liquid Laser Results.

The laser was then operated at 10 Hz with flowing liquid at a pump setting of 60 percent and 1000 J/pulse input. Threshold was just obtained with an average output power of 40 mw. After about one half minute of operation, the flow tube around the pump lamp broke, flooding the area with water. Water pressure forced some water past the laser cell seal and some reaction between the POCl_3 and water took place. The liquid was drained back into its bottle from which slight outgassing occurred for several hours. Examination of the laser cell showed the cell window to be cracked. This probably happened when the flow tube broke and removed the support required for the window to resist the internal pressure.

The accomplishments of this first series of experiments included:

1. Operation of a transverse flowing liquid laser with 10 KW input at a flow rate of 27 gal/min.
2. Successful single shot operation of the transverse flow liquid laser cell at pulse input energies up to 3200 joules.
3. Operation of the mercury wetted pump face seal for several hours without failure.

Problems noted were:

1. The piston pressure compensator became jammed due to precipitation at the seal.
2. Scattering loss in the liquid was high. There were so many particles that the filter quickly became plugged.
3. The pungent odor of the POCl_3 quickly saturates a person's sense of smell for a long period of time. It is not toxic but it is certainly dangerous, as is any acid.
4. Pure POCl_3 will destroy Dow Corning Silastic 733 RTV sealant (the laser liquid will not).

5.2 Second Series of Experiments

The system was cleaned up and completely rebuilt. The pressure compensation piston was removed and the fluid flow path was shortened. Pressure compensation for thermal expansion of the fluid was provided by the gas

pressure in the fill bottle. The rebuilt system is shown in Figure 5-2.

The decision was made to follow a prudent course in the second set of experiments. Experiments were conducted in an order whereby those least likely to damage the system were conducted first and Q-switching experiments were given high priority.

Figures 5-3 and 5-4 show the output pulses obtained with the 24,000 rpm rotating roof prism Q-switch and the static liquid. Input energy was about 1000 joules. Prepulsing occurs with around 100 nsec pulse width due to the slow Q-switching. The final Q-switched pulse is about 45 nsec pulse width and from 4 to 8 M watt peak power, essentially independent of the input pulse energy. The output energy in the last pulse is 200 to 400 millijoules. The prepulse energy can be from 0 to several joules depending on the input energy.

Figure 5-5 shows typical static liquid long pulse output results. Input energy was 1000 joules and output energy was 2.7 joules. The output pulse has considerable spiking with an increasing period between spikes.

The laser was operated at the 1000 joule input level for about one month while testing the Q-switched operation with the rotating roof prism. At the end of this time a static input output energy curve was run with input energies up to 2500 joules. Even though the liquid was of very good optical quality, the results were not as good as those shown in Figure 5-1 for the first series of experiments. For example the output at 2500 joules input was 7.5 joules compared to 10.5 joules in Figure 5-1.

The liquid was then flowed and outgassed using the procedure in Section 4.2. This tremendously increased the scattering loss in the liquid. Static single shot experiments at 1760 joules input produced an output of 0.8 joules compared to 5 joules before flowing the system. Single shot experiments with the liquid flowing at 20 gal/min. produced 0.44 joules at 1760 joules input. Continued flowing of the liquid slowly decreased the

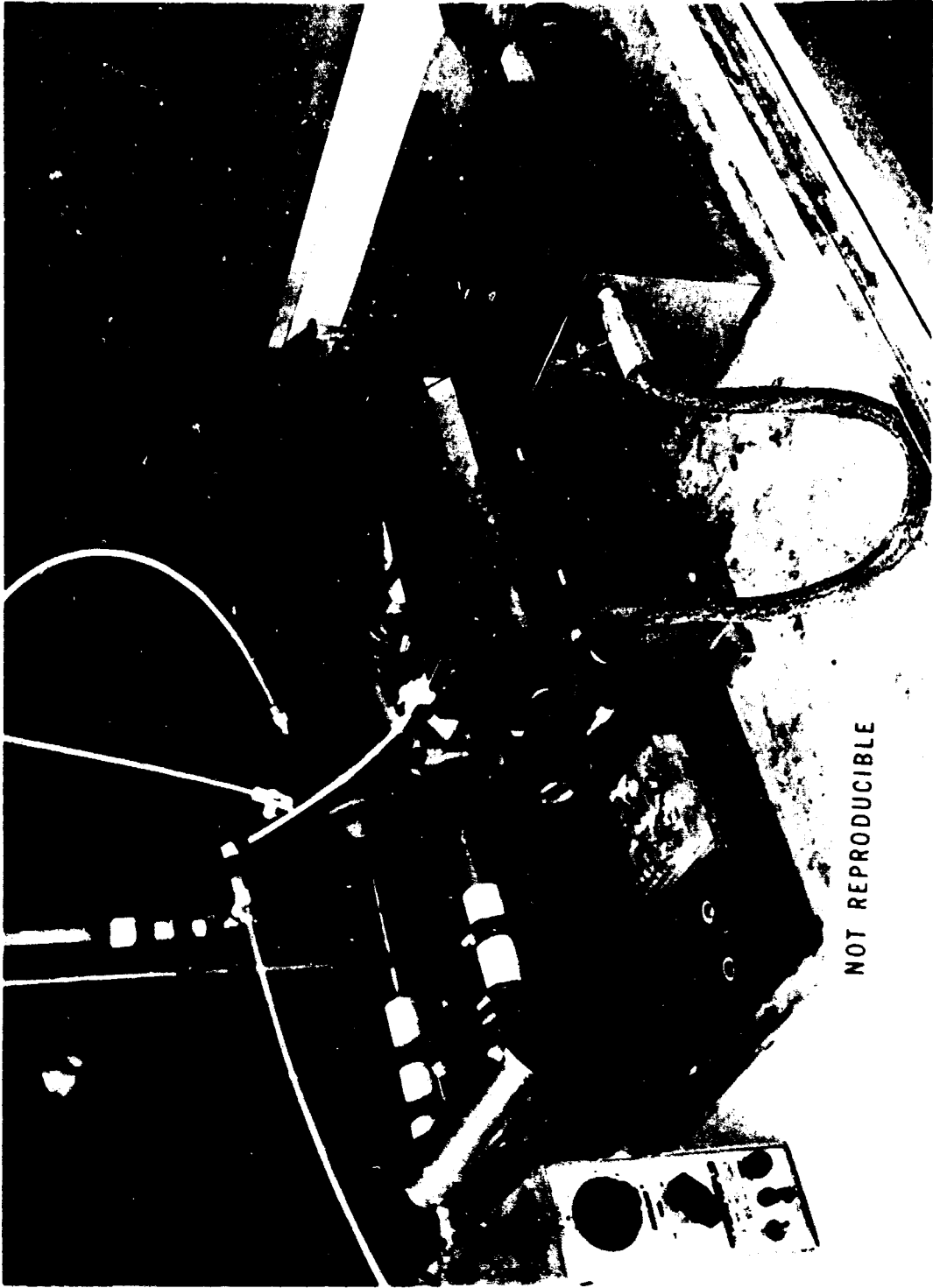


Figure 5-2. Liquid Laser System in Second Series of Experiments.

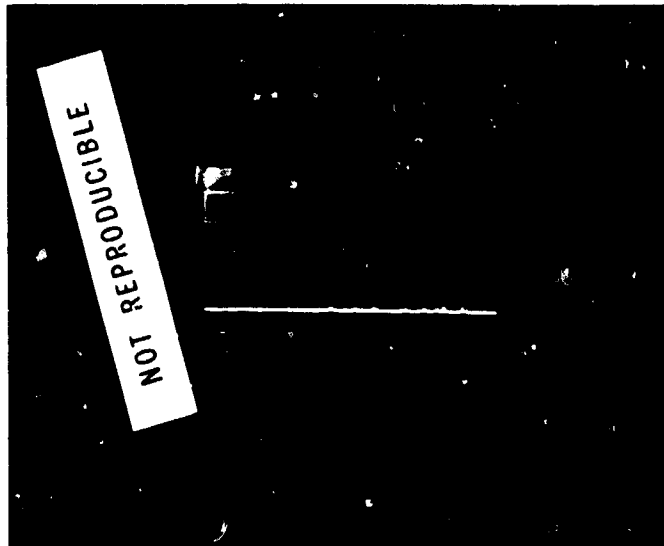


Figure 5-3. Rotating Roof Prism Q-Switch Results for Nd:POCl₃ Liquid Laser. Scale is 4 MW/cm Vertical and 2 μsec/cm Horizontal. Increasing Time for Left to Right.

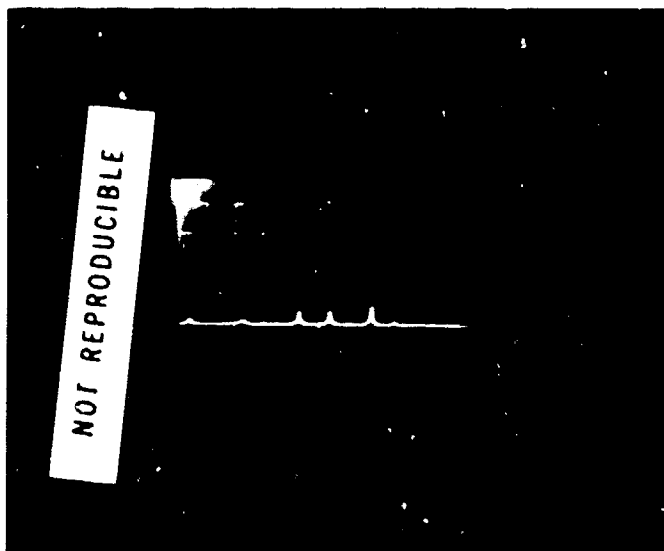


Figure 5-4. Rotating Roof Prism Q-switch Results for Nd:POCl₃ Liquid Laser. Scale is 2 MW/cm Vertical and 1 μsec/cm Horizontal. Increasing Time from Left to Right.

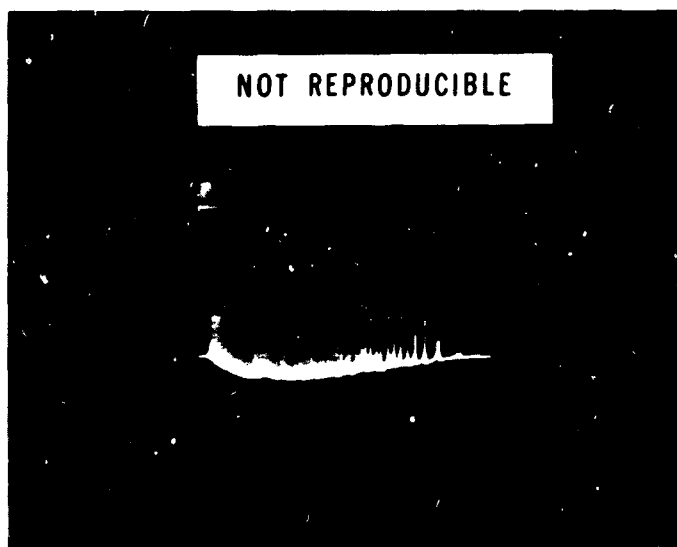


Figure 5-5 Long Pulse Results for Nd:POCl₃ Liquid Laser. Scale in Relative Units Vertical and 50 μ sec/cm Horizontal. Time Increases from Left to Right.

single pulse flowing liquid output. After about 6 hours it had been reduced to 0.28 joules.

It was decided to filter the liquid and inspect the pump cavity reflectors. The gold plated reflectors were found to be badly pitted and flaking. The POCl_3 vapor appeared to have leaked past the liquid seal and corroded the copper plating between the nickel body and the gold plating. This copper is used to increase the adherence of the gold. Figure 5-6 shows the pitted reflectors.

The effects of POCl_3 vapor had been noted for some time by the corrosion of any susceptible material in the area. One particular problem was the anti-reflection coatings on the liquid laser cell end windows. These slowly became flaked and discolored as the experiments proceeded even though they were periodically cleaned.

The system was readied for high repetition rate experiments, but the lamp flow tube was twice broken and no further time nor funds were available to do the experiment. At this time, the system had been filled with the $\text{Nd:POCl}_3:\text{ZrCl}_4$ laser liquid for four months. No deterioration in the fluorescent lifetime of the liquid had occurred. The pump seal still worked properly and would flow the liquid through the system with no liquid leaks at 20 gal/min. flow rate. (Flows greater than 20 gal/min were not used in the second series of experiments to insure that high internal pressures would not break the laser cell side window.)

Accomplishments of the second series of experiments included:

1. Mechanical Q-switched operation at up to 8 MW peak power.
2. No leaks or flow system failures for a four month period.

Problems encountered included:

1. POCl_3 vapor leakage damaged the pump cavity reflectors and the AR window coatings.
2. Scattering buildup in the liquid continued to be a problem. Particles were so numerous that the small bypass filter would be quickly clogged.

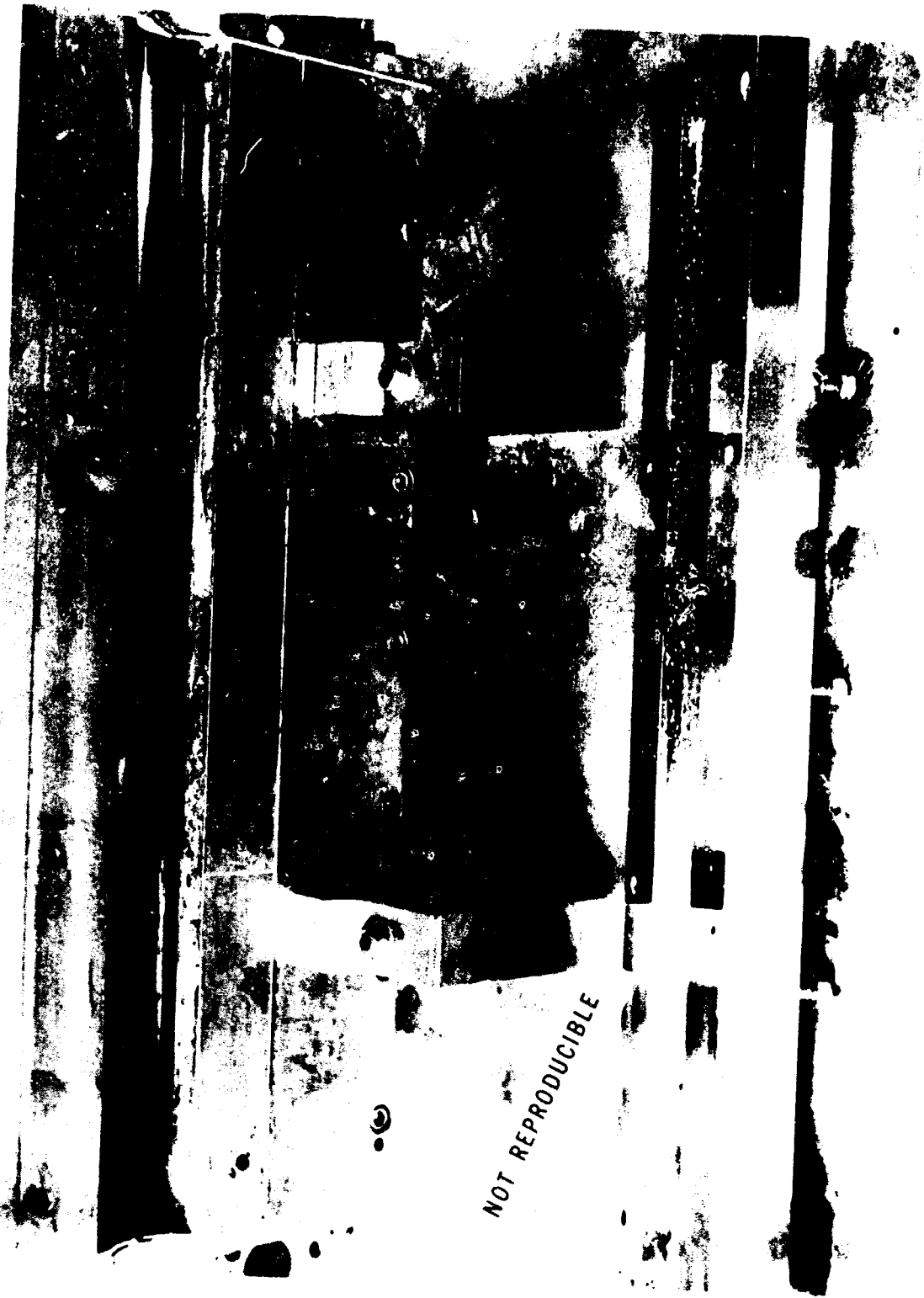


Figure 5-6 Corroded Pump Cavity Reflectors Due to POCl_3 Vapor Leakage
in Liquid Leak Free System

6. CONCLUSIONS AND RECOMMENDATIONS

The corrosive properties and the scattering build up in Nd:POCl₃:ZrCl₄ liquid laser solution are more difficult problems to handle than was anticipated at the start of this program. In particular the construction of a transverse flow system for this liquid is very difficult.

GTE Laboratories have solved many of the corrosion problems with their longitudinal flow laser cell¹⁰. The much simpler and smaller seals required for longitudinal flow are the reason this can be accomplished. GTE Labs. has also found that much better system drying is required to prevent scattering buildup. After flushing with dry nitrogen, several fills of dry POCl₃ must be placed in the system until no trace of water is found on spectrographic check of the POCl₃.

We have considered using a longitudinal flow cell with the liquid circulation system developed on this program. Figure 6-1 shows the pump characteristics and the system load lines for the longitudinal and transverse flow systems. Flow rates of 29 gal/min can be achieved with the longitudinal flow system. This is sufficient for systems of 500 watts and less of average power output.

We still feel that transverse flow liquid lasers have potential of very high output powers. The material problem we have had cause us to recommend the longitudinal flow systems be perfected before further work on transverse flow is attempted, however.

The rotating prism Q-switches were too slow to effectively Q-switch the liquid laser. We recommend that a flowing dye cell be used in conjunction with the roof prism to increase the switching speed. This technique has recently been shown to work.²⁶ We do not recommend electro-optic Q-switches because of surface burning problems.

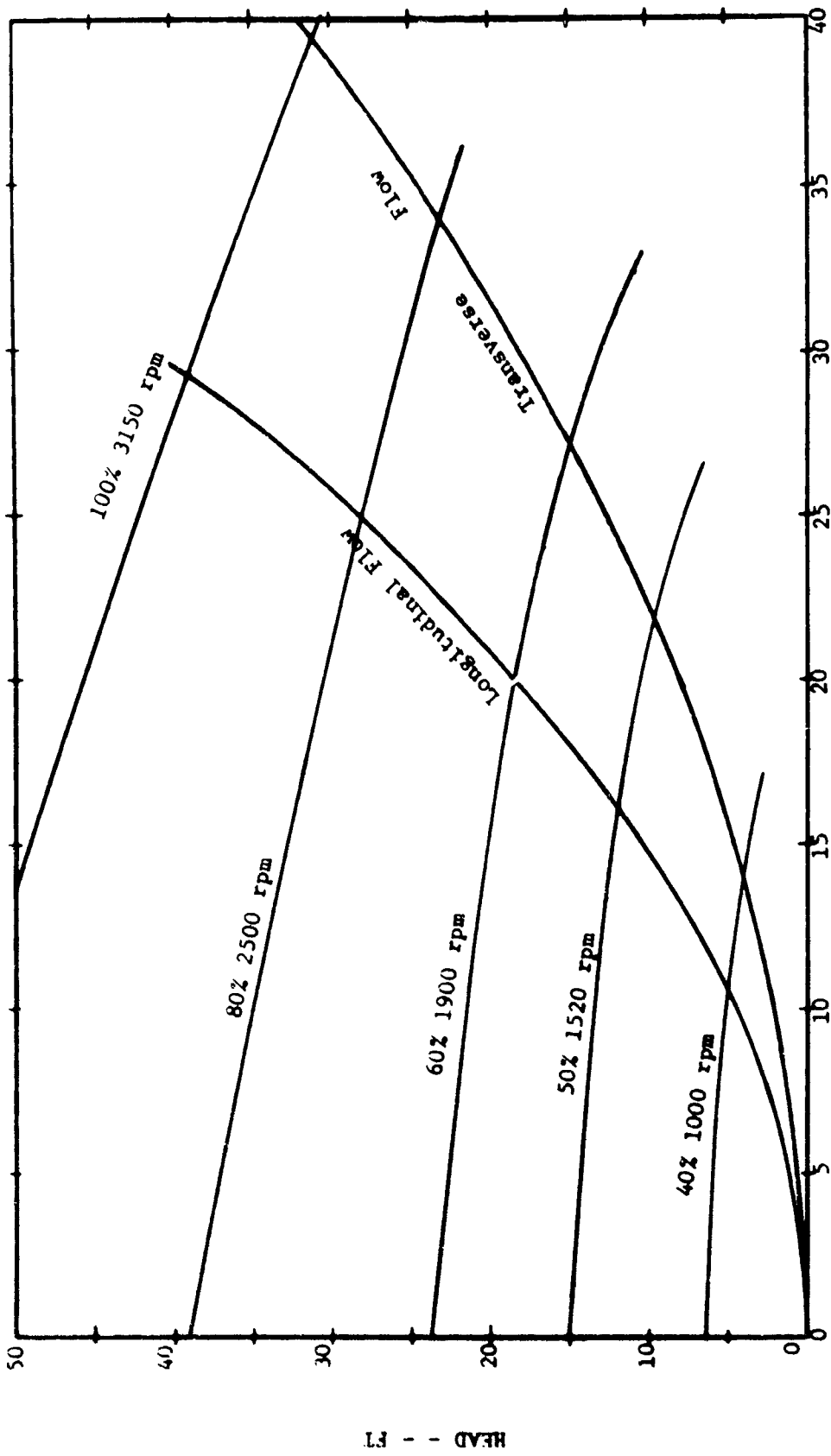


Figure 6-1 Pump Characteristics and System Load Line for Longitudinal Flow and Transverse Flow

We recommend that a longitudinal flow Nd:liquid laser be developed and tested. This laser should be made up of the following components:

1. The liquid flow system developed on this contract.
2. The longitudinal flow cell design developed at GTE Labs.
3. A flowing dye Q-switch⁽²⁶⁾.
4. The double elliptical pump cavity design of the GTE Sylvania Model 612 200 watt Nd:YAG Laser.

These individually proven components should, in combination, provide a system, whereby the great potential of the Nd liquid laser can be realized.

7. REFERENCES

1. A. Heller, "A high Gain Room-Temperature Liquid Laser: Trivalent Neodymium in Selenium Oxychloride," Appl. Phys. Lett. 9, 106, (1 Aug 1966).
2. A. Lempicki and A. Heller "Characteristics of the Nd⁺³:SeOCl₂ Liquid Laser," Appl. Phys. Lett. 9, 108, (1 Aug 1966).
3. M. Y. Zhabotinskiy, N. M. Zhavoronkov, V. G. Lebedev, V. N. Malyshev, Y. P. Rudnitskiy, and G. V. Ellert, "Liquid Lasers," Vestnik AN SSSR, 39, pp 52-57 (Feb 1969).
4. P. M. Buzhinskii, M. E. Zhabotinskii, N. M. Zhavoropkov, V. G. Lebedev, B. I. Malyshev, Y. P. Rudnitskii, V. V. Tsapkin and G. V. Ellert, "Active Materials for Laser Generators and Amplifiers on a Phosphorous Compound Base," Doklady AN SSSR, Vol. 185, No. 6, pp 1306-1308, (June 1969).
5. E. J. Schimitschek, "Laser Emission of a Neodymium Salt Dissolved in POCl₃," J. Appl. Phys. 39, 6120, (Dec. 1968).
6. E. J. Schimitschek, to be published.
7. H. Samelson, A. Lempicki, C. Brecher, R. Kocher, R. R. Alfano, and S. L. Shapiro, "High Energy Pulsed Liquid Laser," Annual Technical Summary Report TR70-826.10, ONR Contract N00014-68-C-0110 (30 Jan 1970).
8. W. R. Watson, A. Lempicki, and S. Reich, "Neodymium Inorganic Aprotic Liquid Laser," Final Report AFAL-TR-69-13, Contract No. F33615-67-C-1580, Air Force Avionics Laboratory, WPAFB, Ohio, (Dec 1968).
9. A. Lempicki, W. R. Watson, and J. Lech, "Neodymium Doped CW Liquid Laser," Final Report AFAL-TR-70-183, Contract No. F33615-69-C-1700, Air Force Avionics Laboratory WPAFB, Ohio, (Aug 1970).
10. H. Samelson, A. Lempicki, R. Kocher, "High Energy Pulsed Liquid Laser," Semiannual Technical Summary Report TR71-826.2, ONR Contract N00014-68-C-0110 (28 Feb 1971).
11. J. D. Foster, and L. M. Osterink, "Thermal Effects in a Nd:YAG Laser," JAP, Vol. 41, pp 3656-3663, (Aug 1970).
12. W. B. Tiffany, R. Targ, and J. D. Foster, "Kilowatt CO₂ Gas-Transport Laser," Appl. Phys. Lett. 15, 91, (1 Aug 1969).
13. W. Rigrod, "Gain Saturation and Output Power of Optical Masers," J. Appl. Phys. 34 2602 (Sept 1963).
14. E. R. Thornton, W. D. Fountain, G. W. Flint, and T. G. Crow, "Properties of Neodymium Laser Materials," Appl. Opt. 8, 1087 (June 1969).

15. The cross section for Nd:YAG is estimated to be $5.7 \times 10^{-19} \text{ cm}^2$ based upon measurement of the saturation parameter β in CW Nd:YAG lasers.
16. Data obtained from manufacturer.
17. Private communications with Dr. A. Lempicki GT&E and Dr. E. Schimitschek NELC.
18. C. Brecher, K. French, W. Watson, and D. Miller, "Transmission Losses in Aprotic Liquid Lasers," JAP, Vol. 41, pp 4578-4581, (Oct 1970).
19. H. Samelson, A. Lempicki, C. Brecher, R. Kocher, R. R. Alfano, and S. L. Shapiro, "High-Energy Pulsed Liquid Laser," Annual Technical Summary Report TR70-826.10 ONR Contract N00014-68-C-0110 (30 Jan 1970).
20. A. Yariv, QUANTUM ELECTRONICS, Wiley and Sons, New York, 1967.
21. L. M. Osterink, "High Average Power Frequency Doubling Laser," Quarterly Report Contract No. F08605-69-C-0054, Patrick Air Force Base, Florida (1 Oct 1969).
22. W. H. McAdams, HEAT TRANSMISSION, McGraw Hill, 1954.
23. Marks, Mechanical Engineers Handbook, 6th Edition, McGraw Hill, 1958.
24. J. P. Markiewicz and J. L. Emmett, IEEE, J. Quant. Elec. QE2, 708 (Nov 1966).
25. R. C. Benson and M. R. Mirarchi, "The Spinning Reflector Technique for Ruby Laser Pulse Control," IEEE Trans. Mil. Elec. MIL-8, 13, (Jan 1964).
26. A. R. Clobes, M. J. Brienza, "Pulsed Nd:YAG Laser Utilizing a Flowing Dye Cell," J. Quant. Elec., QE-6, 651 (Oct. 1970).
27. D. G. Carlson, "Dynamics of a Repetitively Pump-Pulsed Nd:YAG Laser" JAP, 39, pp. 4369-4374 (Aug 1968).